METHODS FOR MEASURING THE THERMAL CONDUCTIVITY OF EARTH MATERIALS WITH APPLICATION TO ANISOTROPY IN BASALT AND HEAT FLUX THROUGH LAKE SEDIMENTS

by

George P. Watts

METHODS FOR MEASURING THERMAL CONDUCTIVITY OF EARTH MATERIALS WITH APPLICATION TO ANISOTROPY IN BASALT AND HEAT FLUX THROUGH LAKE SEDIMENTS

A THESIS SUBMITTED TO THE GRADUATE DIVISION OF THE UNIVERSITY OF HAWAII IN PARTIAL FULFILLMENT OF THE REQUIREMENTS FOR THE DEGREE OF

MASTER OF SCIENCE

IN GEOLOGY AND GEOPHYSICS

AUGUST 1975

By

George Patrick Watts

Thesis Committee:

William M. Adams, Chairman
Frank L. Peterson
Murli H. Manghnani
Alfred H. Woodcock

We certify that we have read this thesis and that in our opinion it is satisfactory in scope and quality as a thesis for the degree of Masters of Science in Geology and Geophysics.

THESIS COMMITTEE

William Mansfield Adams

Chairman

Frank L. Pitt

Murli H. Manghnani

Alfred H. Woodcock

ACKNOWLEDGEMENTS

It gives me much pleasure to extend gratitude to those who have assisted with this study. David Epp provided me with assistance in the construction of the steady-state apparatus, direction in the needle-probe measurements and guidance to relevant literature. Dr. K. A. Pankiwskyj graciously gave me useful advice and references pertaining to the petrology of my rock specimens. Advice from Dr. G. A. Macdonald on geological aspects of the study has been most helpful.

I also owe much gratitude to George Mason for his programming assistance, Daniel Palmiter for his thin-section analysis of my rock specimens, Dr. G. Uehara for the use of the soil physics laboratory, and Alex Nakamura of NOAA for the use of equipment. Financial support has been provided, in part, by NSF grant GF-42982, and by supplies from the Department of Geology and Geophysics, University of Hawaii.

ABSTRACT

In the geophysical exploration of geothermal reservoirs, the most reliable indicator of a heat deposit is the direct indication of a low heat flux associated with a high geothermal gradient. Any alternative geophysical indicator is less reliable, being indirect. For example, a map of temperature, or geothermal gradient, may be confounded by variations in thermal conductivity. The determination of heat flux requires knowing both the thermal conductivity and the vertical gradient of temperature. This study reports on laboratory measurements of the thermal conductivity of basalt, and the determination of the thermal conductivity of sediments beneath an alpine lake on the volcano, Mauna Kea from field measurements of temperature.

For the laboratory work, a factor of thermal conductive anisotropy of 0.78 is found in a specimen from the Sugarloaf lava flow on the island of Oahu.

An improved procedure is developed for analyzing temperature data from relatively shallow bore holes (less than 20 meters in depth). The method is applied to the data from lake sediments, temperature versus depth over time, giving as an estimate of the thermal diffusivity 0.00212 cm^2/sec. This estimate is further utilized to find the thermal conductivity, 0.00205 cal/sec cm °C, and the heat flux, 1.07 μcal/sec cm^2, downward in the sediments of Lake Waiau on the island of Hawaii.

TABLE OF CONTENTS

Page

LIST OF TABLES

LIST OF ILLUSTRATIONS

Chapter 1

THERMAL CONDUCTIVITY IN GEOTHERMAL EXPLORATION

Most geothermal phenomena in the continental land masses of the earth's crust may be treated theoretically by the laws of heat conduction. Over the water-covered areas of the earth's crust, in ground-water domains and in active magma movements heat transfer by convection plays a dominant role. Convection processes are of special interest in applied geothermal exploration methods because they create the geothermal conditions that serve as an indication of moving ground water or, in volcanic areas, give rise to exploitable heat sources. It is the purpose of this study to investigate the significance of thermal conductivity in geothermal exploration. Future studies could be directed towards the influence of thermal convection in geothermal exploration as a sequel to this work.

The economic importance of the earth's heat as a source of energy has been proven by the successful geothermal power plants located in Italy, New Zealand and the United States, reported by McNitt (1965). Hammond, et al. (1973) summarize the types of geothermal resources that are currently being exploited as well as those that are being researched for exploitation within the United States. They consider three types of geothermal resources in their study; steam, hot water and hot rock. Steam is the most widely exploited of these three resources. Hot water is much more abundant than steam, but has been successfully exploited only by a couple of countries. Even larger resources of hot rock are available, however, their exploitation has not yet been proven technically feasible.

At sufficient depths, hot rock exists everywhere and a capable technology would make it a most appealing energy resource. For the present, research is limited to shallow intrusions as sources of hot rock. D. Blackwell has discovered a potential hot rock source near Helena, Montana, reported by Cowan (1974). This hot dry rock is thought to have the highest known heat flow rate in the United States and it is currently being researched for development.

The criteria for defining an economically exploitable geothermal resource for the present time are listed by Adams (1975) as follows.

1. The temperature should be greater than 200°C (about 400°F).
2. There must be water available at this temperature.
3. The hot water (or steam) should occur in a relatively permeable stratum to permit efficient transfer of energy to a point of withdrawal.
4. The relatively permeable stratum should be capped by a relatively impermeable stratum to prevent the casual escape and spacial spreading of the concentrated energy.
5. The volume of rock of the permeable stratum (or reservoir stratum) should be greater than 100 cubic kilometers (a cube of about 5 kilometers on a side).
6. The bottom of the impermeable stratum should be at a depth less than two kilometers.
7. The reservoir should be in a location such that the electrical energy produced can be tied into an electrical distribution system economically.

The geothermal gradient is the measured difference in temperature

per unit vertical distance within earth materials. An exploitable geothermal resource as described above will display a geothermal gradient of around 130°C per 100 meters in the overlying rock and soil. This geothermal gradient is about six or seven times the normal gradient and according to Kappelmeyer and Haenel (1974, p. 141) it is used as the principle indicator in geothermal exploration methods.

Kappelmeyer and Haenel (1974, p. 142) describe three types of geothermal-gradient measurements currently used in geothermal exploration: soil-temperature measurements made in bore holes with depths of about two to five meters, shallow bore holes to depths between 50 to 200 meters, and deep wells down to about 1500 meters. The present practice of geothermal exploration includes making thermal-conductivity measurements solely on selected samples from the deep wells. Thermal conductivity is the physical property that controls the rate of heat transfer through the material.

If a geothermal gradient were measured in a shallow bore hole or from soil probes, there is always the question of how deep it can be extrapolated. The measurement could be anomalously high for a number of reasons. One reason is evident in the following situation. If two identical heat deposits are each beneath a column of material with a different thermal conductivity from the other column, the geothermal gradient will be higher in the column with the smaller thermal-conductivity value after a significant time lapse. Thus the heat deposit overlain by low conducting material would have a greater lifetime and be considered more elgible as an economically exploitable source of heat.

It is therefore very desireable to know the thermal conductivity of the materials from which the geothermal gradients were measured. Consequently, the heat flux, the rate of heat flow per unit area, is the most reliable indicator of a geothermal reservoir since it includes the thermal conductivity of the materials involved. The second chapter offers a review of the theory of thermal conductivity in nonmetallic solids.

The first part of this study is to illustrate an inexpensive steady-state method to obtain reliable thermal-conductivity values to complement geothermal-gradient measurements from shallow bore holes and soil-temperature probes. The third chapter describes the design of the apparatus and the steady-state method of measuring thermal conductivity including a test measurement of glass. Chapter 4 is an application of the method described. Core samples from the Sugarloaf lava flow were measured at different orientations. The purpose is to evaluate the effects that the cooling of a thick layer of molten lava would have on the thermal properties of the rock mass. A search of the literature did not reveal any reference to a determination of anisotropic thermal conductivity in basalt.

The second part of the study describes an improved method for determining the thermal conductivity of soil from temperature probes. Chapter 5 reviews the various nonsteady-state methods of determining thermal conductivity used in this study. The sixth chapter demonstrates the improved nonsteady-state method as it is applied to temperature measurements in the sediments of Lake Waiau. Chapter 7 includes the measurements of core samples from Lake Waiau with the steady-state appara-

tus described in Chapter 3 as a comparison of the methods developed for boths parts of this study. Also in this chapter is the final determination of the first 'in situ' thermal conductivity made in Hawaii for geothermal applications with a heat-flux calculation for the sediments of Lake Waiau.

Chapter 2

THEORY OF THERMAL CONDUCTIVITY

There are three distinct modes of heat transfer: conduction, convection and radiation. Thermal conduction occurs by means of lattice vibrations in a body. Thermal convection applies to heat that is being transferred by the relative motion of portions of the body. Thermal radiation refers to heat moved between distant parts of the body by electromagnetic radiation. Conduction is the primary mode of heat transfer through solid bodies in the physical state encountered in this study. Convection is most important in liquids and gases, and is present in solid materials under high temperatures and pressures. Radiation is usually negligible in solids, except at high temperatures. In geothermal-exploration studies of heat-flux anomalies within crustal materials, we are primarily concerned with lattice conductivity.

Heat in solids is conducted by various carriers. In metals and alloys the free electrons are important carriers of heat. However, in nonmetallic solids, the equalization of temperature averages takes place mostly through lattice interaction, or the interaction of molecules, and in many cases these lattice vibrations are the only carriers.

Lattice Conductivity.

An atom displaced about its equilibrium position within the lattice of a solid is subject to a restoring force proportional to its displacement and will undergo a simple harmonic motion. The neighboring atoms with which this atom is coupled by interatomic binding forces are also set into such a motion. Oscillation of the neighboring atoms causes

the disturbance within the crystal to be propagated as an elastic wave. These elastic waves are referred to as lattice vibrations, or phonons.

In Debye theory, the lattice vibrations are described as being anharmonic, and this anharmonicity provides the coupling, or scattering, between waves that cause thermal resistance. At high temperatures, greater than 300°K for most earth materials, each atom or molecule can be said to vibrate independently of its neighbors, and the lattice vibrations are highly coupled and are best described by elastic waves in a continuum. For the temperatures encountered in this study, the lattice vibrations are to be considered dispersive.

Fourier's Law.

Conductive heat-transfer is founded upon a fundamental hypothesis, called Fourier's Law. The concept is best visualized through the following description presented by Carslaw and Jaeger (1959). Suppose a plate of solid material is bounded by two parallel planes each of which is maintained at constant and different temperatures. These planes should cover enough area to appear infinite in extent relative to the center portion. After sufficient time lapse, temperature equilization approaches completeness throughout the plate, and is referred to as steady-state heat flow. Figure 2-1 shows the situation described.

Only a small cylindrical section in the plate of solid material is considered in the hypothesis. The cross-sectional area, A, of the surface adjacent to the planes is expressed in cm^2, and the separation, z, in cm is the distance between the planes. The heat flow within the cylinder is only along the cylindrical axis which is normal to the

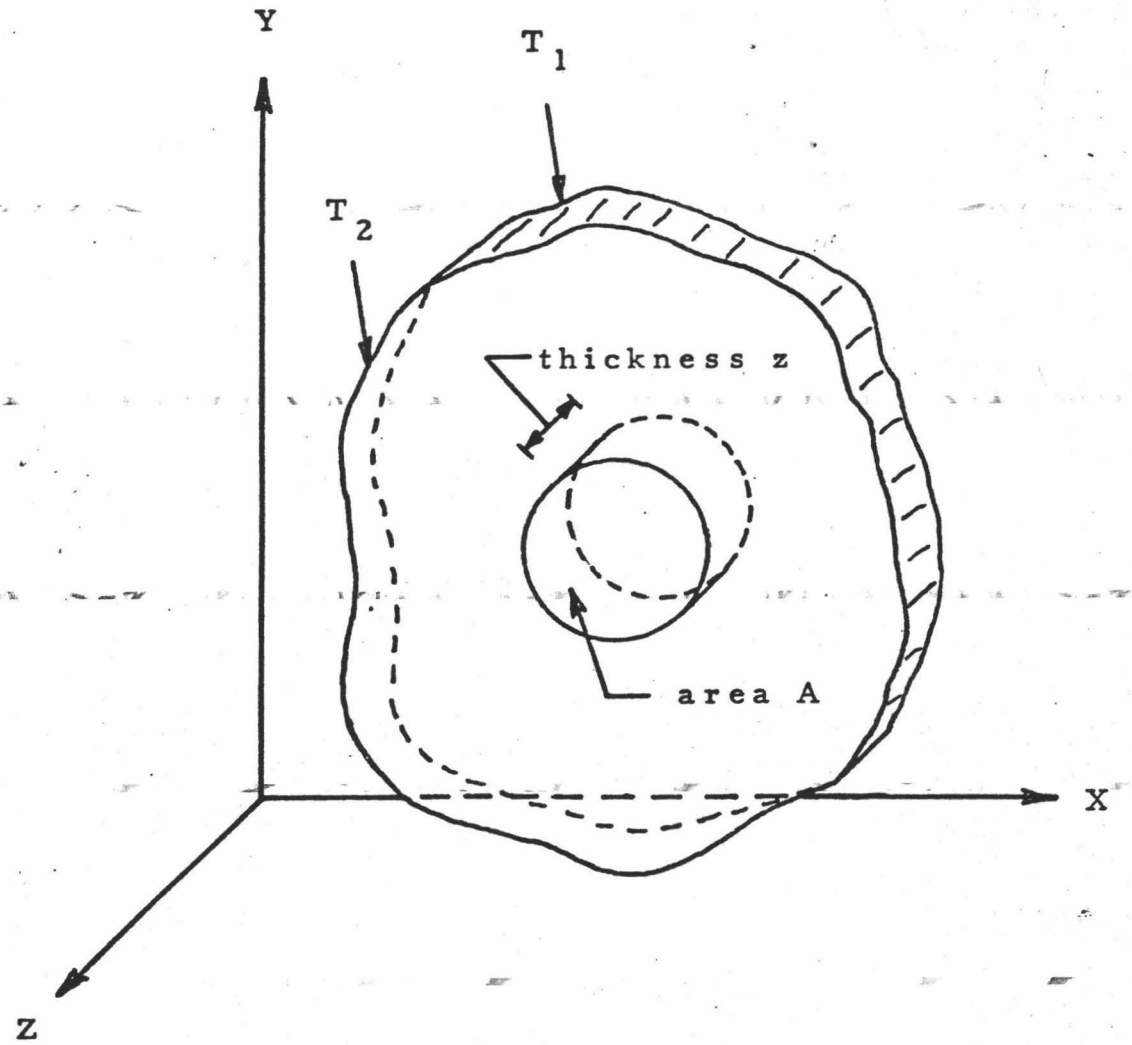

Figure 2-1. Schematic diagram of the geometry assumed in Fourier's Law.

bounding planes. The expression defining the quantity of heat, Q, in calories, that flows through the cylinder is given by Fourier's Law

$$Q = k(T_2 - T_1)At / z \tag{2.1}$$

where T_1 and T_2 are the temperatures of the bounding planes in °C, t is time in sec, and k is a property depending upon the material of the plate called the thermal conductivity.

If we let q = Q/t represent the rate of heat flow, then the thermal conductivity from equation (2.1) can be expressed as

$$k = qz / A(T_2 - T_1) \tag{2.2}$$

where the dimensions of k are calories per centimeter per second per degree centigrade.

Heat Conduction in Isotropic Media.

An isotropic medium is one whose structure and properties in the neighborhood of any point within the medium are independent of the direction through the point. The heat flux, $\vec{f}$, is a vector quantity given in the relation

$$\vec{f} = Q / At\,\vec{n} \tag{2.3}$$

and defined as the flow of heat per unit time per unit area in a given direction, where $\vec{n}$ is the unit vector normal to A in the direction of decreasing temperature.

If a medium is defined by a rectangular coordinate system and temperature changes occur along the z-axis only, then the xy-planes will be isothermal planes. At a distance z + dz, the temperature will be T - dT, if the direction of heat flow is along the positive z-axis. The quantity dT/dz is called the thermal gradient, and has dimensions of degrees cen-

tigrade per centimeter in the cgs system. An xy-plane at a distnace, z, from the origin will have the amount of heat flowing through unit area and in unit time given by

$$\vec{f}_z = - k \, (dT/dz) \, \vec{1} \qquad (2.4)$$

where $\vec{1}$ is the unit vector in the z direction.

Heat Conduction in Anisotropic Media.

In anisotropic media the direction of the heat flux vector at a point is not necessarily normal to the isothermal surface through the point. If we assume each component of the heat flux vector to be linearly dependent on all components of the thermal gradient at a point, Fourier's Law for heterogeneous anisotropic material becomes

$$\begin{aligned} \vec{f}_x &= -(k_{11}(\partial T/\partial x)\vec{i} + k_{12}(\partial T/\partial y)\vec{j} + k_{13}(\partial T/\partial z)\vec{1}) \\ \vec{f}_y &= -(k_{21}(\partial T/\partial x)\vec{i} + k_{22}(\partial T/\partial y)\vec{j} + k_{23}(\partial T/\partial z)\vec{1}) \\ \vec{f}_z &= -(k_{31}(\partial T/\partial x)\vec{i} + k_{32}(\partial T/\partial y)\vec{j} + k_{33}(\partial T/\partial z)\vec{1}) \end{aligned} \qquad (2.5)$$

where $\vec{i}$, $\vec{j}$ and $\vec{1}$ are the unit vectors in the x, y and z directions respectively. Thus, k is a tensor of the second order.

In isotropic layers, where the thermal conductivity is different in three mutually perpendicular directions, which are taken as the x, y and z axes, the set of equations (2.5) reduces to

$$\begin{aligned} \vec{f}_x &= - k_1(\partial T/\partial x)\vec{i} \\ \vec{f}_y &= - k_2(\partial T/\partial y)\vec{j} \\ \vec{f}_z &= - k_3(\partial T/\partial z)\vec{1}. \end{aligned} \qquad (2.6)$$

If the thermal conductivity is independent of direction in the xy-plane and has a different value on the perpendicular to this plane, equations (2.5) become

$$\vec{f}_x = - k_{11}(\partial T/\partial x)\vec{i}$$
$$\vec{f}_y = - k_{11}(\partial T/\partial y)\vec{j} \qquad (2.7)$$
$$\vec{f}_z = - k_1(\partial T/\partial z)\vec{1}.$$

This form is valid for most layered sediments, and is often referred to as transverse anisotropy.

Relation of Thermal Conductivity to Temperature.

Thermal conductivity is a physical quantity dependent on the chemical composition of the material constituting the medium as well as on its physical conditions, such as temperature and porosity. The temperature range encountered in this study is very limited, 0-100°C. The thermal conductivity of some materials, such as fused quartz, have some small temperature dependence within this temperature range. Sugawara (1968) gives

$$k = a + bT \qquad (2.8)$$

as an empirical thermal conductivity-temperature relationship. The temperature dependence is very small for most earth materials within this temperature range.

Effect of Water Content on Thermal Conductivity.

The water content in earth materials has been found to vary the thermal conductivity considerably. Horai and Uyeda (1960) have studied this effect. Figure 2-2 is a graph of their thermal-conductivity measurements of shale specimens with varying water content. A maximum occurs at approximately 16% (weight percentage) water content.

Their interpretation is that the thermal conductivity in the water-

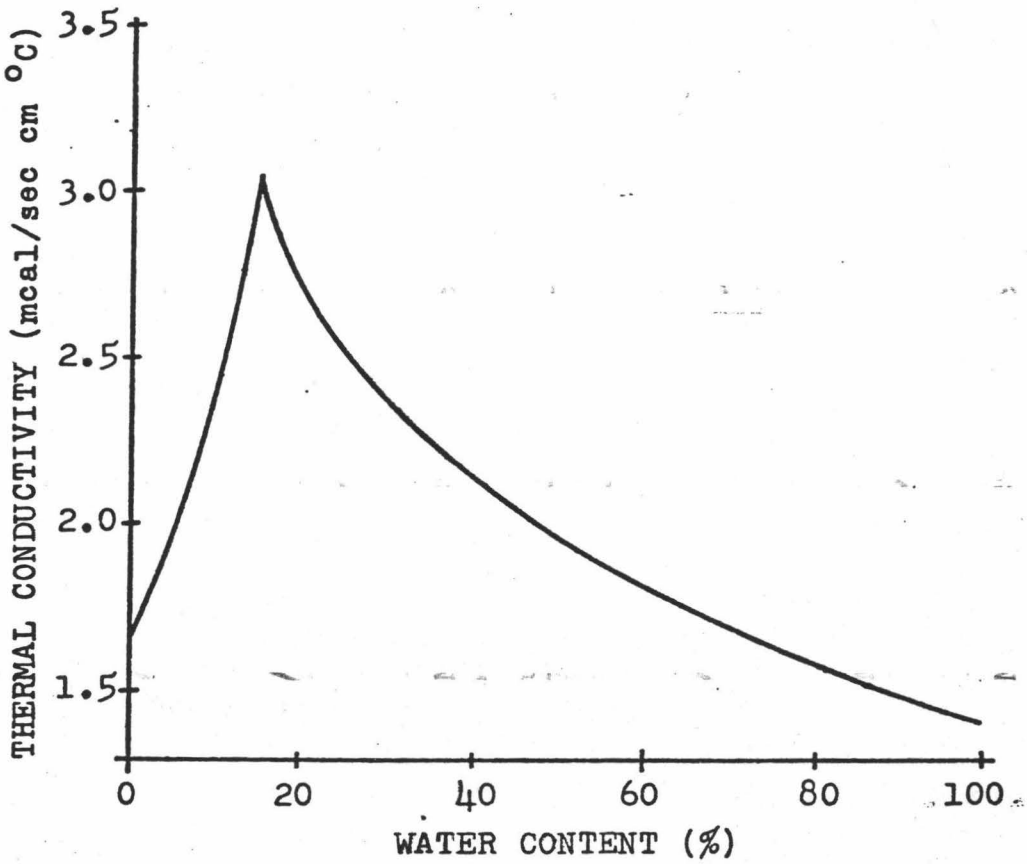

Figure 2-2. Relation between thermal conductivity of shale samples and water content (weight percentage), after Horai and Uyeda (1960).

rich region decreases with increase of water content because the solid particles having a greater thermal conductivity than water are more and more replaced by water. While in the water-poor region, the decrease in thermal conductivity with decrease of water content is caused by substitution of water by the air, a poorer conductor of heat.

Part I

LABORATORY STEADY-STATE METHOD FOR THE MEASUREMENT OF THERMAL CONDUCTIVITY

Chapter 3

STEADY-STATE MEASUREMENT OF THERMAL CONDUCTIVITY

For a complete description of heat flux distribution, the thermal conductivity of the materials involved must be known. Laboratory measurements of the thermal conductivity of rocks can be made by both steady-state and nonsteady-state methods. Steady-state methods are impractical for field measurements and one has to use nonsteady-state methods for 'in situ' measurements. The steady-state laboratory method is described below. The test specimen is subjected to a temperature difference across two opposite surfaces and the thermal conductivity is determined directly by measuring the rate of heat flow per unit area through the specimen together with the temperature gradient across it after equilibrium has been reached. Equilibrium refers to the steady-state condition when the temperature difference across the specimen is no longer varying over time.

Even though the apparatus built for this study was designed to utilize the steady-state method, it can also use the nonsteady-state method, with the temperature distribution varying with time, to measure thermal diffusivity from a longitudinal periodic heat flow. This is an indirect method of obtaining values for thermal conductivity since measurements or estimates of specific heat and density are also required. This method is described by Abeles, et al. (1960) and others. Chapter 5 includes a more complete description of nonsteady-state methods.

Description of Apparatus.

Figure 3-1 is a schematic diagram of the apparatus used in this

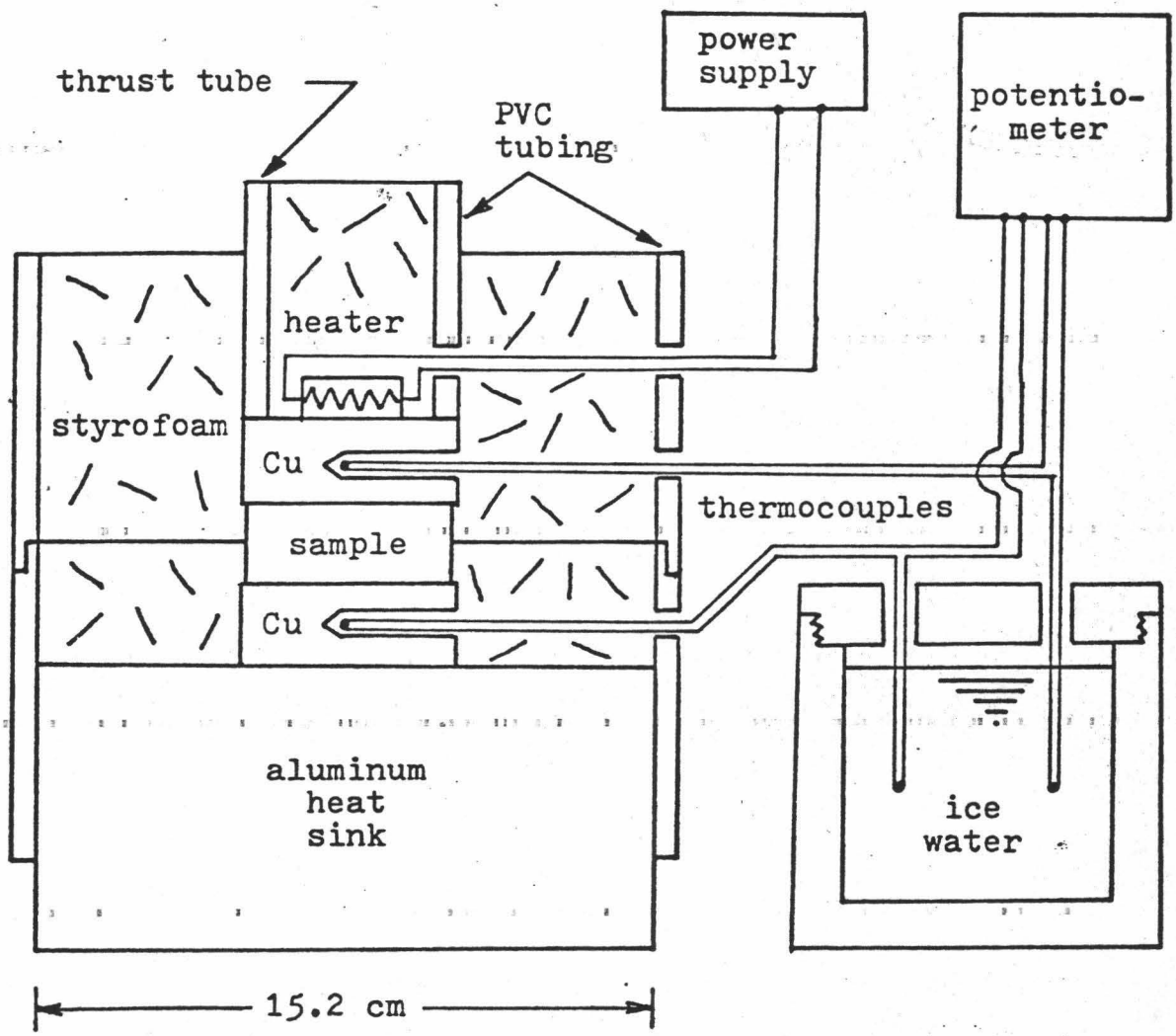

Figure 3-1. Diametrical cross-section of steady-state apparatus for measuring thermal conductivity.

study, a modified design of an apparatus built by Birch (1940). The geometry of the apparatus is axi-symmetric and the heat flow is longitudinal along the axis. Discs, about 5 cm in diameter, sliced from core samples, are the specimens measured in this apparatus. The apparatus was used for making measurements of thermal conductivity for poor conductors. The design differs from an apparatus that measures good conductors in that the specimen length is much shorter for poor conductors. This is needed to minimize the radial heat loss and to shorten the time required to reach equilibrium.

The apparatus is similar to the one described by Reiter and Hartman (1971). They used a screw press to apply axial pressure on the specimen, while my apparatus uses a 15.2 kg weight to maintain a constant axial stress of 0.73 bars on the specimen. The specimen can be subjected to greater stresses by using a hydraulic press. Figure 3-2 is a photograph of the apparatus in operation.

The apparatus contains two copper discs with the specimen disc sandwiched between. Figure 3-3 is a photograph of the separated apparatus. The heating element is a wire-wound resistor, having resistance of about 5 ohms, and is attached to the upper copper disc. The lower copper disc is seated upon a massive aluminum heat sink. The oven is encased in a section of 6-inch polyvinyl chloride pipe (PVC). The thrust tube, also a section of PVC pipe, 1.5 inches in diameter, is attached to the upper copper disc and supports the 15.2 kg weight during the measurements. The PVC pipes are molded with styrofoam to provide thermal insulation.

Touloukian, et al. (1970) recommend a value for the thermal conduc-

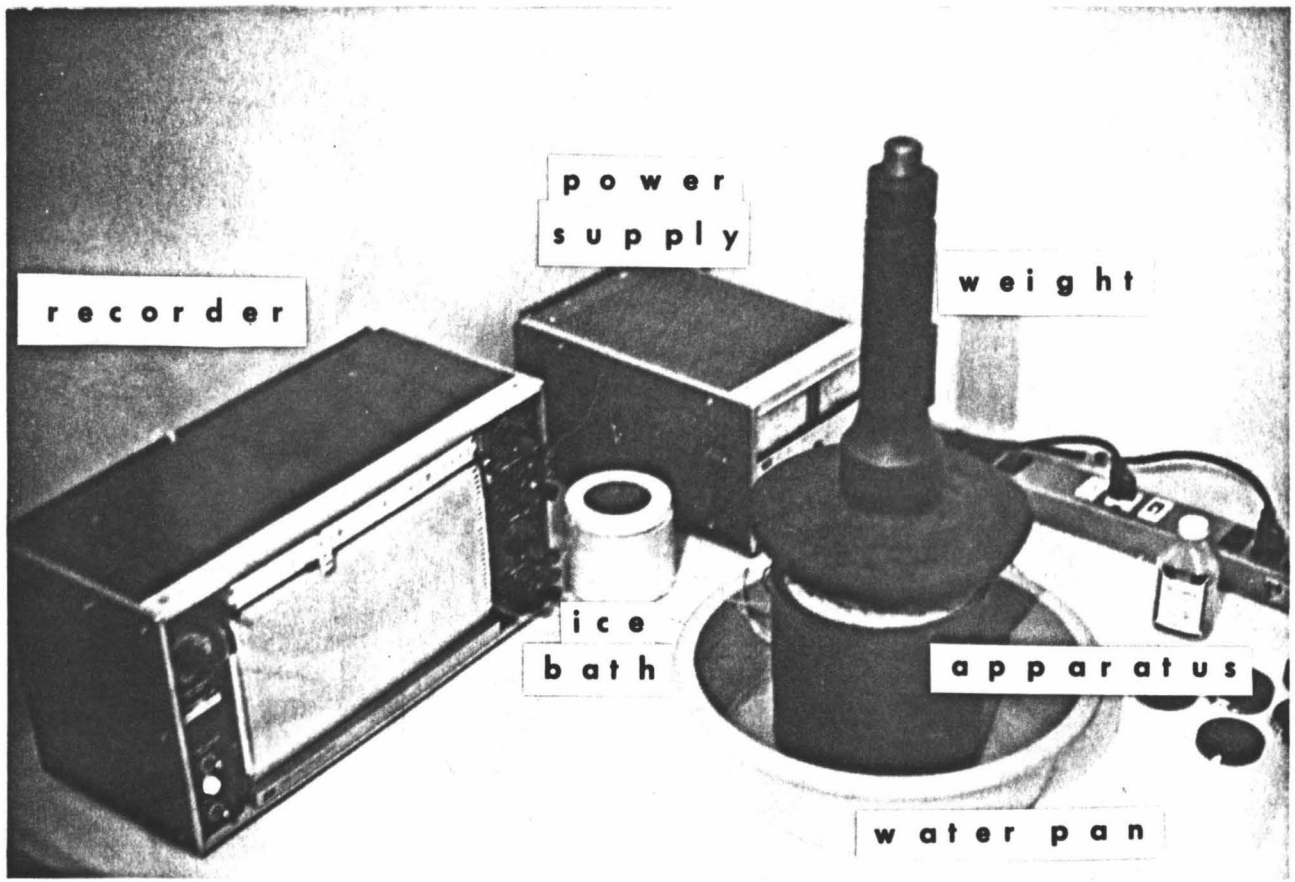

Figure 3-2. The steady-state thermal conductivity measuring apparatus shown in operation.

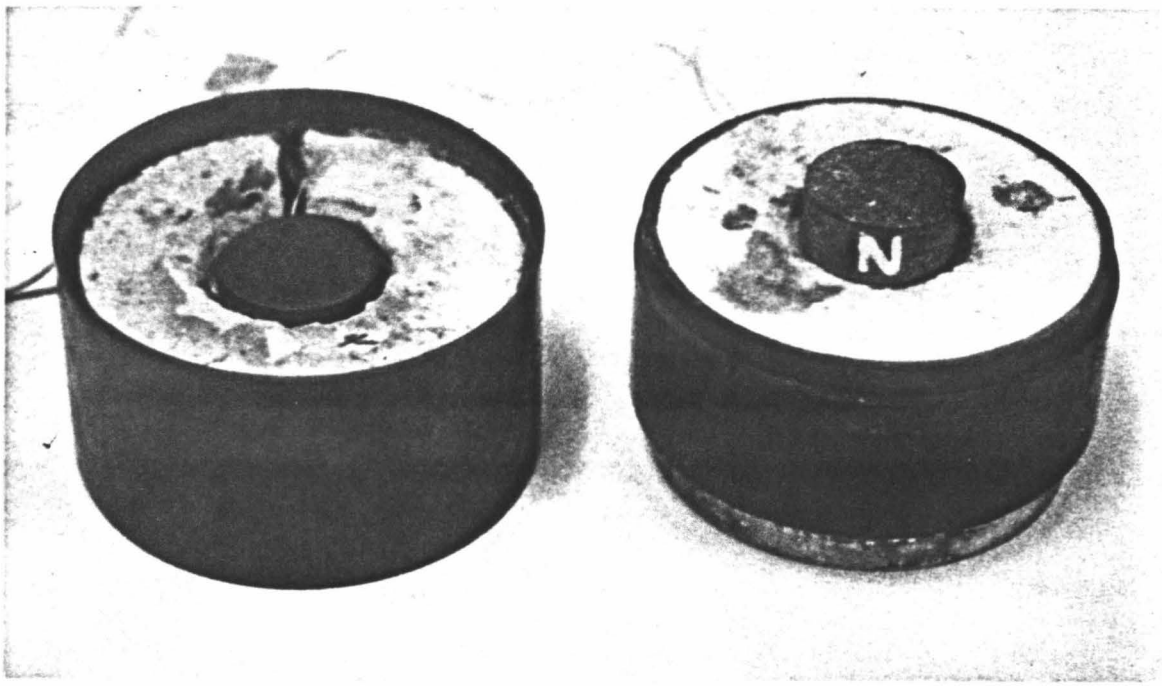

top bottom

Figure 3-3. The steady-state thermal conductivity measuring apparatus with the encasement oven separated to show the specimen's position.

tivity of 99.999+% pure copper at 300°K is 0.951 cal/sec cm °K. They also recommend for 99.9999% pure aluminum at 300°K a value of 0.566 cal/sec cm °K. Their measurements show the value for polyvinyl chloride (PVC-I) at 303°K to be 0.000330 cal/sec cm °K. The thermal conductivity of styrofoam varies more with the packing density than with temperature. It was therefore necessary to measure the thermal conductivity with a needle probe. The needle-probe method of thermal-conductivity measurement is a transient method, which is described and discussed further in Chapter 5. The mean of four independent measurements is 0.000133 cal/sec cm °K for the molded styrofoam.

Figure 3-4 is a schematic model of the relative thermal-conductivity boundaries of the materials comprising the apparatus. The copper discs have a radius of 2.54 cm and are 1.93 cm in thickness. The sample disc is assumed to have similar dimensions with a thermal conductivity near 0.003 cal/sec cm °K. Table 3-1 shows a numerical representation of the interfaces offering the least resistance to the flow of heat through each of the three discs. If we assume that all of the heat from the heater passes into the upper copper disc, then it is apparent from Table 3-1 that most of the heat will flow across the sample-copper interface. Even lesser amounts of heat are lost as it passes through the sample disc and the lower copper disc into the aluminum heat sink. An estimate of the error produced by these losses is offered later in this chapter.

The heat sink was placed in a pan of water at room temperature, and the temperature was monitored for several hours during an experiment; only minor variations occurred. The operational procedure included the

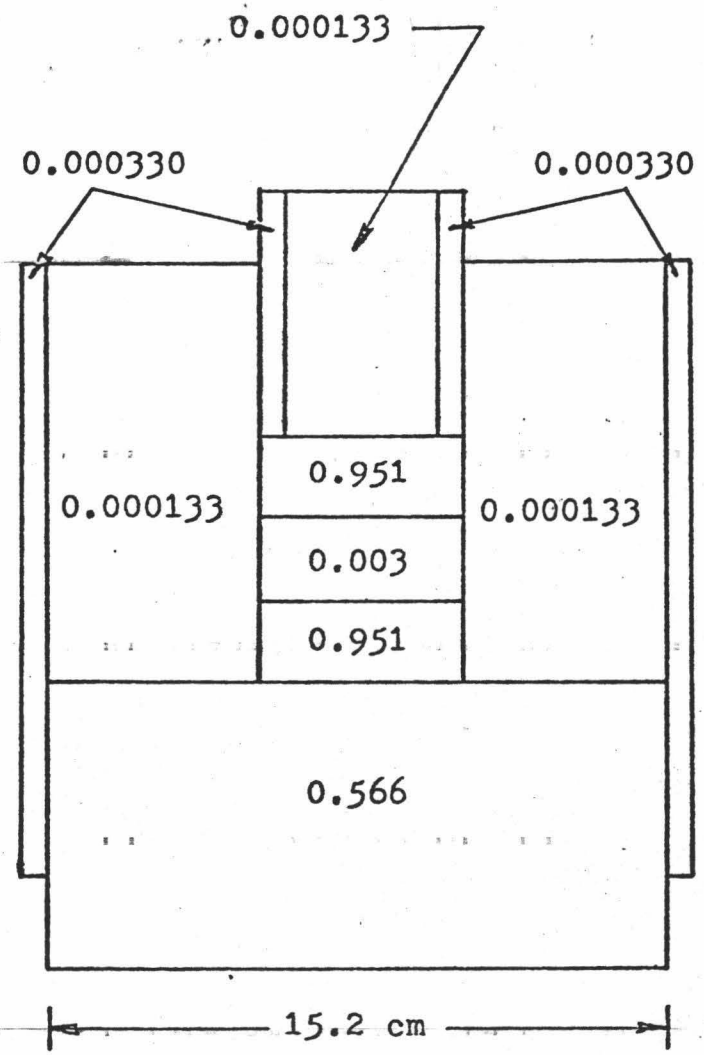

Figure 3-4. Schematic model of thermal conductivity interfaces of steady-state apparatus. Dimensions are cal/cm-sec °C.

Table 3-1. List of relative contact surface-areas with corresponding thermal-conductivity ratios for every interface of the three discs within the steady-state apparatus.

Disc	Interface	Percent of Disc's Total Surface Area	Thermal-Conductivity Ratio
	PVC/Copper	8.7	0.000347
Upper Copper	Styrofoam/Copper	62.9	0.000140
	Sample/Copper	28.4	0.00315
	Copper/Sample	28.4	317.0
Sample	Styrofoam/Sample	43.2	0.0443
	Copper/Sample	28.4	317.0
	Sample/Copper	28.4	0.00315
Lower Copper	Styrofoam/Copper	43.2	0.000140
	Aluminum/Copper	28.4	0.595

pan of water to expand the heat capacity of the thermal sink. The heat input from the heat sink to the sample would result primarily from ambient fluctuations and can be considered experimentally insignificant. For a single specimen, about half of the measurements were made with the water at room temperature and half were measured with ice in the water pan, thus providing measurements at two levels of temperature.

Both copper discs are bored, and each has the measuring junction of a chromel-constantan thermocouple inserted into the borehole. The reference junctions of these thermocouples are submerged in an ice-water bath during the measurements.

Explanation of Measurement Procedure.

In this longitudinal heat-flow method, the experimental arrangement is so designed that the flow of heat is only in the axial direction of a disc specimen. The radial heat-loss from the specimen is minimized greatly. Under steady-state conditions, and assuming no radial heat-loss, the thermal conductivity is determined by the following expression from the one-dimensional heat conduction equation

$$k = (q/A) \; / \; (\Delta T/\Delta z) \qquad (3.1)$$

where k is the thermal conductivity (heat flow per unit time per unit distance per degree of temperature) corresponding to the temperature $(T_1+T_2)/2$, $\Delta T = T_2-T_1$, q is the rate of heat flow, A is the cross-sectional area of the specimen, and Δz is the distance between points of temperature measurement for T_1 and T_2. From equation (3.1), the parameters needed to solve for k are the heat flux, q/A, (heat flow per unit time per unit area) through the specimen and the temperature gradient,

$\Delta T/\Delta z$, (change in temperature per unit distance) across the specimen. The thermal conductivity of the specimen is obtained by dividing the heat flux by the temperature gradient.

The heat flow is hampered by the contact resistance at the interface between two bodies causing errors in the temperature measurements. Glycerin was applied to the circular surfaces of both sides of the copper discs to minimize this problem. The axial pressure applied on the discs also facilitated a good thermal contact.

Determination of the Heat Flux.

If we know the power output of the heater, we can divide by the surface area of the specimen to obtain the heat flux. A stable power supply must be used to maintain a constant source of heat. The power to the heater was provided by a Hewlett-Packard dual D.C. power supply, model 6227B, with a specified stability of less than 0.2% plus 2 mv total drift for 8 hours.

The power output of the heater is equivalent to the energy dissipated by it, which is the same as the heat flow per unit time from the heater. The power, q, in cal/sec, is then determined by measuring the voltage, V, across and the current, i, through the heater and using the conversion relation $q = iV / 4.1858$. Thus, the heat flow determination is independent of the resistance of the heater. The operational procedure included keeping the current set to 1 ampere with the voltage constant at 5 volts.

The diameter of the specimen was measured to the nearest 0.05 mm with a vernier caliper. From this measurement the surface area of the

specimen was readily calculated. The heat flux was obtained by dividing the power, as defined in the preceding paragraph, by the cross-sectional area of the specimen.

Determination of Temperature Gradient.

The thickness, Δz, of the specimen was obtained using a Zues micrometer, which enabled measurement to the nearest 0.01 mm, and using the method suggested by Misener and Beck (1960) to determine the flatness of a specimen. The mean value of 6 measurements taken around the edge is used if it doesn't differ from the value measured at the center by more than 0.03 mm.

The temperature difference, ΔT, across the specimen was determined by measuring the voltages across chromel-constantan thermocouples. The voltages were measured using a potentiometer consisting of two Hewlett-Packard input modules, model 17505A, and a dual-channel Hewlett-Packard strip-chart recorder, model 7100BM-19-23. The manufacturer's specifications cite an accuracy of $\pm$ 0.0125 mv at a voltage span of 5 mv.

The thermocouples were constructed using chromel (nickel-chromium alloy) and constantan (copper-nickel alloy). The chromel-constantan thermocouples are unique in having the highest emf output of any standard metallic thermocouple. The thermocouple voltage measurements are converted to temperatures using the calibration tables made available by the National Bureau of Standards in 1971. The Omega Engineering catalog cites the limit of error for chromel-constantan thermocouples as $\pm$ 0.21 °C in the temperature range of 0-300°C. The temperature gradient, in °C/cm, was determined by dividing the temperature difference across the

specimen by the thickness of the specimen.

Sensitivity Analysis.

A sensitivity analysis of the measurement equation, $k=qz/A(T_2-T_1)$, was made following the method described by Tomovic (1963, p. 25). The sensitivity is a measure of the amount by which the thermal conductivity, k, differs from its nomial value when one of its measurement parameters differs from the number chosen as its nomial value. The mathematical model, $F(k,x)=0$, is used where x is one parameter in the measurement equation. The static sensitivity coefficient is $u(x)=(-\partial F/\partial x)/(\partial F/\partial k)$.

The evaluation of the heat flow, q, gave a sensitivity coefficient of $u(q)=k/q$. This implies the obvious, that the thermal conductivity varies directly with the heat flow. The heat flow was maintained by a stable power supply within the limits 1.194 - 1.199 cal/sec for all measurements. Therefore, the worst case for the heat flow measurement could cause an error of 0.2% in the thermal conductivity computation. The specimen thickness, z, is also directly proportional to the thermal conductivity. The thickness was measured within ±0.001 cm. This measurement could cause a worst case error of 0.07% in the thermal conductivity measurement.

The surface area, A, of the specimen gave a negative sensitivity coefficient, $u(A)=-k/A$, indicating the thermal conductivity varies inversely with the surface area. The area was obtained by measuring the diameter of the specimen within ±0.005 cm. The worst case error of 0.0001% in the area measurement would have a negligible effect on the thermal conductivity determination.

The temperature difference, (T_2-T_1), across the specimen was evaluated to have a sensitivity coefficient of $u(T_2-T_1) = -k/(T_2-T_1)$. Each temperature was measured to within ± 0.21 °C. If T_2 and T_1 were close to each other in value, a sizeable sensitivity error could exist. This would be the case in the measurement of good conductors with this apparatus. The materials measured in this study maintained a temperature difference around 15°C at steady-state. Therefore, a worst case error of 2.6% could exist in the thermal-conductivity value due to the lack of sensitivity in the temperature measurements.

The worst possible case of the sensitivity error for a thermal-conductivity measurement of a material with a thermal conductivity similar to fused quartz with this apparatus would then be the sum of the above errors, which is 2.9%. It is apparent from the above analysis that the voltage and current measurements are the sensitivie parameters in the calculation. In particular, the voltages that determine the temperature difference are the most sensitive parameters and require the most care in their measurement.

Measurements on Fused Quartz.

Silica glass (fused quartz) is an isotropic and homogeneous material having thermal-conductivity values similar to many rock types. The thermal conductivity of fused quartz has been measured by many scientists who were interested in thermal conductivities of rocks and other poor conductors, with apparatus similar to the one built for this study. Satisfactory agreement among these measured values has not been achieved. Figure 3-5 is a composite graph of thermal conductivity versus tempera-

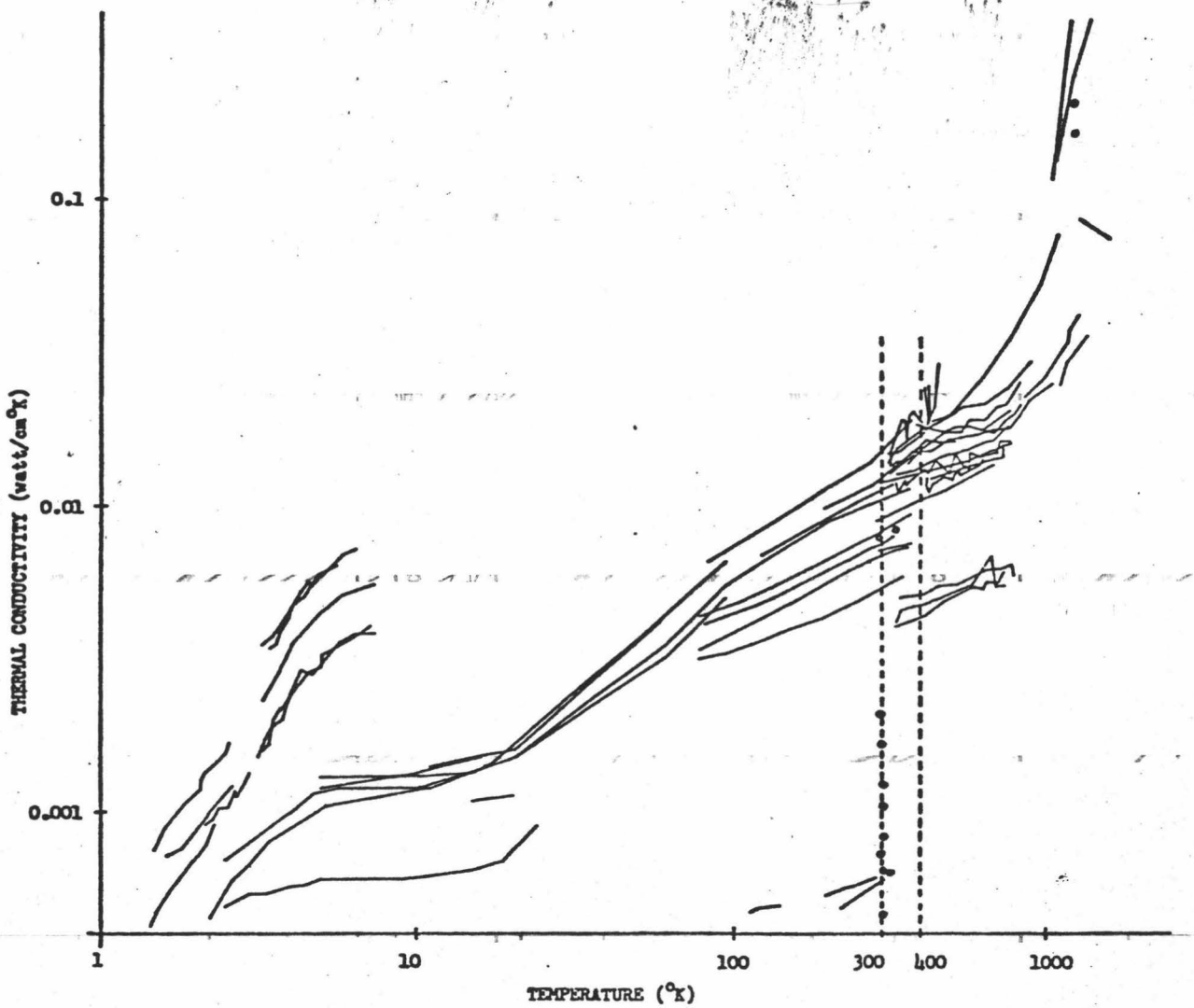

Figure 3-5. Measurements from many investigators of the thermal conductivity of fused silica plotted against temperature, after Touloukian, et al. (1970). The temperatures 300°K and 400 °K bound the range encountered in this study.

ture for many of these investigations. Very few of these investigators state the purity of their samples, therefore, it is difficult to assess the variations in the measurements.

Much effort has been made by Sugawara (1968) to standardize the thermal conductivity of 99.97% pure fused quartz for calibration purposes. His results are

$$k = 3.22 + 0.0042\ T \qquad (3.2)$$

in the temperature range 0-50°C, where k is the thermal conductivity (mcal/sec cm °C) and T is the mean temperature (°C) of the sample. Sugawara states the accuracy of his measurements are within 1.5% of the true value.

A sample of glass was obtained from the glass blower at the Chemistry Department of the University of Hawaii. The chemical composition of the specimen is unknown.

This sample was measured independently 25 times in the temperature range of 25-50°C. These measurements are listed in Table 3-2. A least squares regression line was computed to fit the thermal conductivity values to the sample mean-temperature values, shown in Figure 3-6. The regression equation from the computation is

$$k = 3.06 + 0.0088\ T \qquad (3.3)$$

where k has the same dimensions as equation (3.2). The standard error of the estimate is 0.076 and the mean reproducibility error of this experiment is calculated to be 1.81%. The 90 percent confidence interval has been computed for equation (3.3) and is plotted on Figure 3-6.

Equation (3.3) differs from equation (3.2) by 1.4% at 25°C and 2.0% at 50°C. A crossover occurs near 35°C, shown in Figure 3-7. The close-

Table 3-2. Thermal conductivity measurements on glass specimen.

Date	Time of Day	Ambient Air Temperature (°C)	Sample Mean Temperature (°C)	Thermal Conductivity (cal/sec cm °C)
12Jun74	----	----	42.53	0.0034
15Jun74	----	----	43.24	0.0034
17Jun74	----	----	40.45	0.0035
22Jun74	----	----	43.32	0.0034
25Jun74	----	----	43.83	0.0034
29Jun74	----	----	43.16	0.0034
3Jul74	1830	----	46.46	0.0034
4Jul74	1130	----	44.43	0.0033
4Jul74	1600	----	43.25	0.0035
6Jul74	1700	----	47.90	0.0035
7Jul74	1400	----	46.12	0.0035
8Jul74	1800	----	46.60	0.0035
11Jul74	1645	29.1	48.97	0.0035
11Jan75	1230	26.6	29.50	0.0032
12Jan75	0610	23.9	41.93	0.0035
12Jan75	1345	25.3	43.69	0.0035
12Jan75	1930	24.8	42.36	0.0035
17Jan75	2100	26.5	34.46	0.0033
18Jan75	0600	25.6	29.23	0.0034
18Jan75	1400	26.6	29.01	0.0032
18Jan75	1845	27.3	27.07	0.0034
18Jan75	2130	25.8	27.64	0.0033
19Jan75	1310	26.5	32.75	0.0033
19Jan75	1600	27.2	28.22	0.0034
19Jan75	1900	27.7	27.84	0.0033

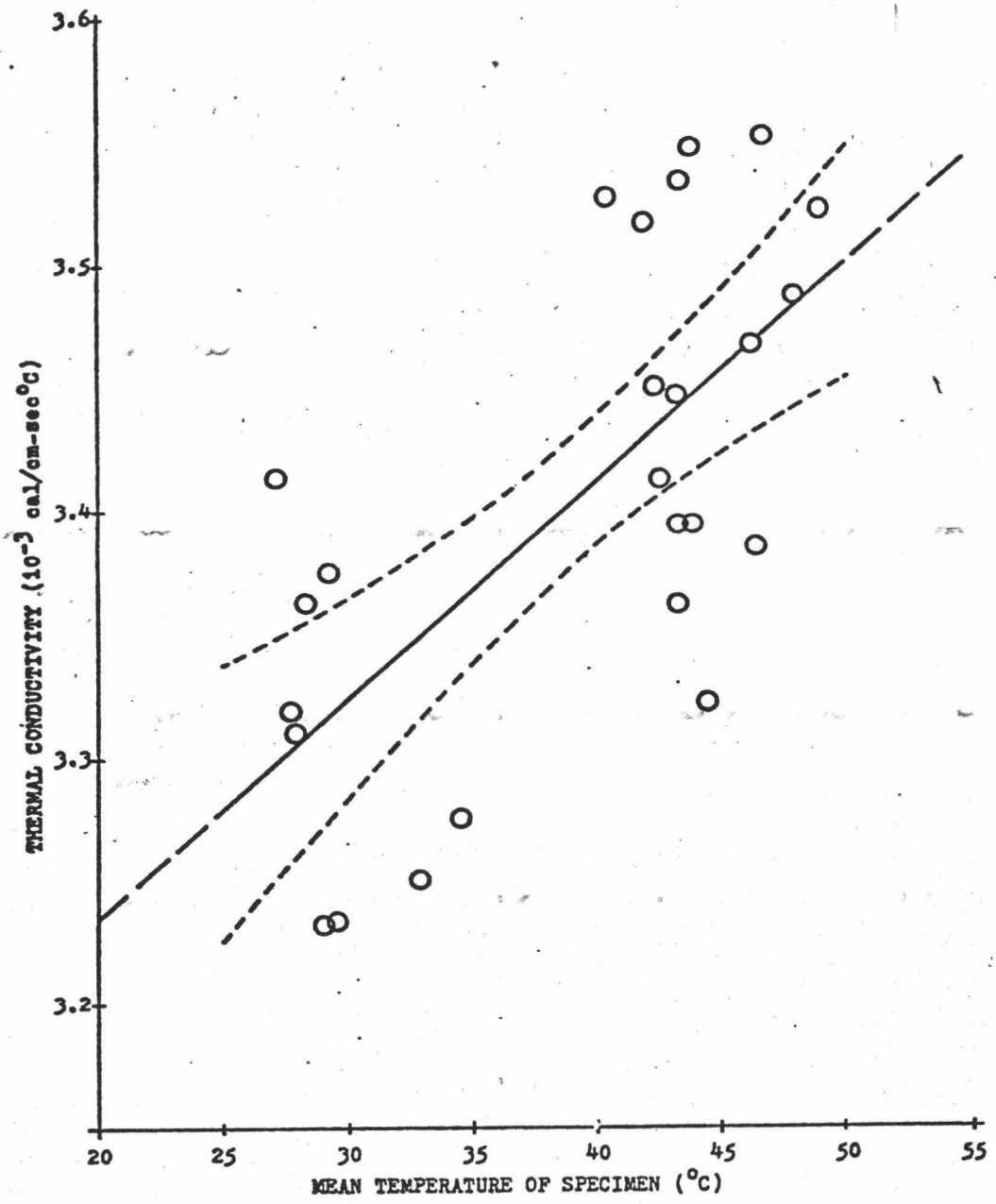

Figure 3-6. Plot of thermal conductivity against temperature for fused quartz measurements. The regression line consists of the thermal conductivity values fitted to the temperature and bounded by the 90% confidence interval.

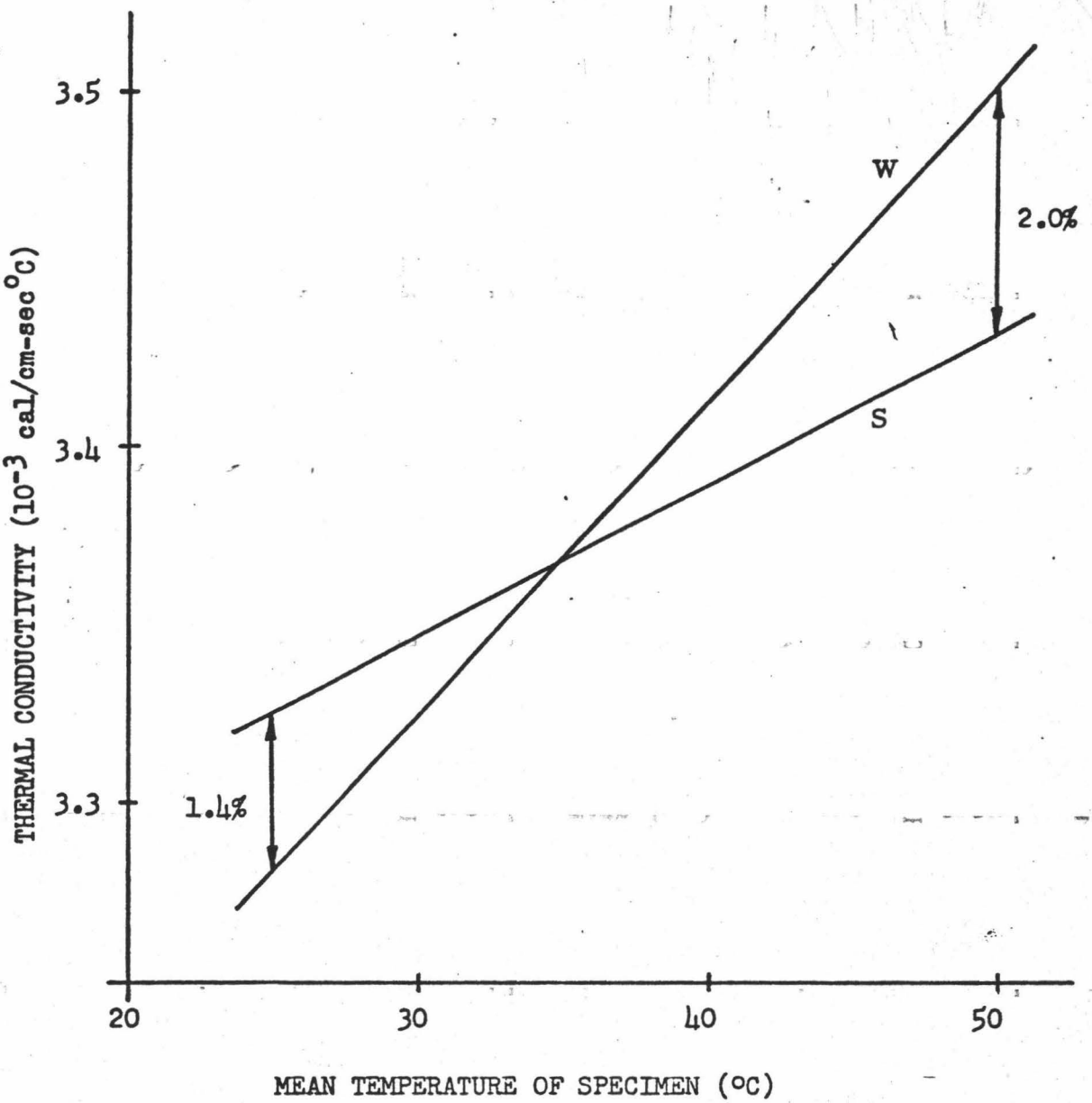

Figure 3-7. Graph of regression line of fused quartz measurements, labeled W, with the measurements obtained by Sugawara (1968), labeled S.

ness of the two measurements suggests that the chemical composition of the two specimens is similar. Thus, the test specimen measured in this study is very likely to have a high quartz content.

Estimation of Heat Loss.

An intuitive insight into the flow of heat through the copper and sample discs inside the apparatus has been presented earlier in this chapter. This analysis is summarized in Figure 3-4 and Table 3-1. An estimate of the radial heat loss and the upward axial heat loss is based on the following assumptions, which are representative of an actual measurement.

1. The time required for the measurement to reach steady-state is 2.5 hours (9000 seconds).
2. The ambient temperature is constant at 25°C.
3. All of the heat from the heater is transferred into the upper copper disc.
4. The temperature of the upper copper disc is maintained at 55°C.
5. The temperature of the lower copper disc is maintained at 30°C.
6. The sample specimen has a thermal conductivity of 0.003 cal/sec cm °C, with a radius of 2.54 cm and a thickness of 1.93 cm.
7. The heat flux into the copper discs and the sample disc is 0.04 cal/sec cm^2.

Figure 3-8 is a schematic diagram of the conditions stated above and the dimensions used in the estimate. The heat loss is a transient process in reality and this estimate is to be considered a first approximation.

The computation of the estimate is made by evaluating the quantity

Ambient Air
Temperature = 25°C

Duration of
Measurement = 9000 sec
($2\frac{1}{2}$hrs)

Radius of Discs = 2.54cm

Heat Flux through
Sample = 0.04 cal/cm^{2}sec

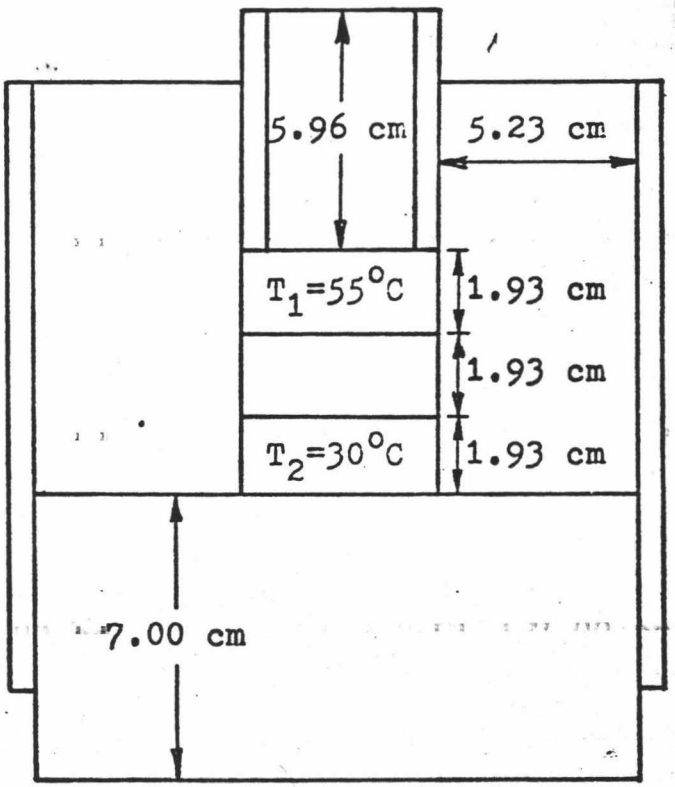

Figure 3-8. Diagram of the dimensions and the assumptions used in the heat loss estimate for the steady-state apparatus.

of heat, Q, that would flow through each surface area, A, of each of the three discs over a period of time, t (2.5 hours), with respect to the thermal conductivity, k, of each contact medium surrounding the disc and the temperature gradient, $\Delta T/\Delta z$, across the contact medium. This is accomplished using the equation

$$Q = k\ At\ (\Delta T/\Delta z) \qquad (3.4)$$

derived from Fourier's Law and the information taken from Figure 3-4 and Figure 3-8.

For the upper copper disc, there are four surface areas pertinent to the computation.

1. The axial heat loss upward to the styrofoam is 95.73 calories.
2. The axial heat loss upward to the PVC thrust tube is 65.47 calories.
3. The radial heat loss to the styrofoam is 67.32 calories.
4. The heat flow into the sample disc is 7088.62 calories.

Compared to the total heat transfer, 3.12% escapes from the upper copper disc, 0.01% is lost to the styrofoam from the sample disc, and 0.02% is lost to the styrofoam from the lower copper disc; a total of 3.15%. This heat loss would tend to increase the measured thermal conductivity because a lesser amount of heat would be flowing through the sample than the measured amount of heat indicates.

Contact Resistance Problem.

The interface formed by the contact surfaces of the copper discs with the sample disc and the aluminum heat sink each represent a resistance to the flow of heat between the adjacent materials. This problem

exists because of microscopic asperities at the interface that constrain the flow of heat to narrow paths across the interface, illustrated in Figure 3-9. No unified theory exists for predicting contact heat transfer and this is due, in part, to the difficulty of trying to describe statistically a contact surface. By adding a liquid film to the contact surface, as in this study, the difficulty in predicting the solid conductance with its many variables is further complicated by the many variables due to the fluid conductance across the interface. However, the heat flux across the interface is greatly increased with the presence of the fluid.

Ratcliffe (1959) gives a method of estimating the error introduced by a liquid film applied to the contact interfaces to reduce contact resistance. If the sum of the film thicknesses on both sides of the sample is small with respect to the sample thicknesses and reproducible for each measurement, then the following equation can be applied

$$z/k = z/k_a - z_f/k_f \tag{3.5}$$

where k is the thermal conductivity of the sample with thickness z, k_a is the apparent thermal conductivity measured, and k_f is the thermal conductivity of the liquid film which has a thickness of z_f. If we let $c = z_f/k_f$, then equation (3.5) reduces to

$$1/k_a = 1/k + c/z. \tag{3.6}$$

Touloukian, et al. (1970) cite the thermal conductivity of glycerin to be 0.0006883 cal/sec cm °K at 300°K. If we assume the thickness of the glycerin film on both sides of the sample to be 0.00254 cm, after Reiter and Hartman (1971), and the sample parameters shown in Figure 3-4 and Figure 3-8 apply, then an error of - 0.6% is introduced by the pre-

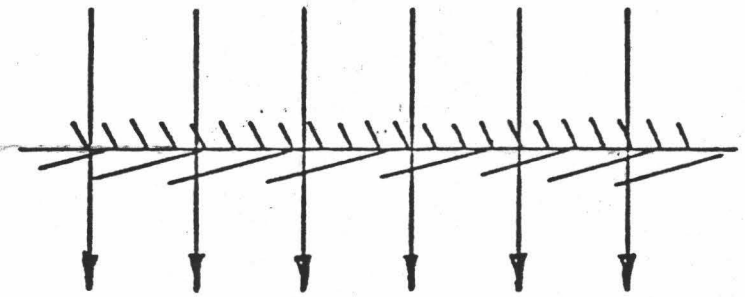

idealized interface

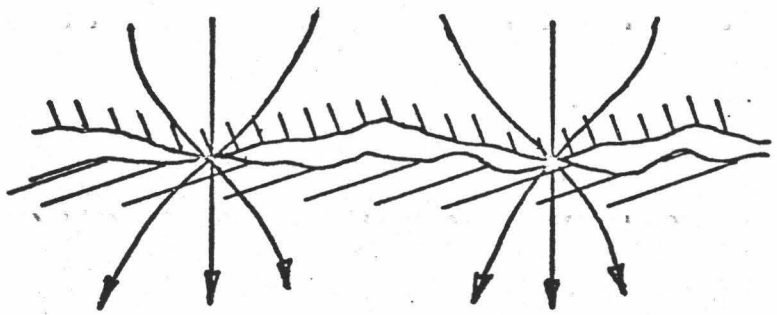

actual interface

Figure 3-9. Heat flux lines at an interface, after Fried (1969).

sence of the glycerin. This error would be many times greater without the glycerin.

The constrained conduction paths at the interface would cause the top surface at each interface to have a higher temperature. The positioning of the thermocouples at the lower portion of the upper copper disc and the upper portion of the lower copper disc would measure a larger temperature gradient than if there were no contact resistance. The presence of contact resistance tends to cause the measured thermal conductivity to be less than the true thermal conductivity.

Chapter 4

ANISOTROPIC THERMAL CONDUCTIVITY IN HAWAIIAN BASALT

Kappelmeyer and Haenel (1974, p. 218) have compiled a list of results from several sources on the anisotropy of thermal conductivity for many rock types. Investigations of anisotropic basalt are absent from this list. A search of the literature also failed to reveal any experimental data concerning thermal conductive anisotropy in basalt.

Sugarloaf is among the row of vents along the ridge of the Koolau Range on the west side of Manoa Valley on the island of Oahu in Hawaii. The most recent flow of lava from Sugarloaf poured out into the lower end of Manoa Valley with a bearing of S12°W in this area. Its thickness is approximately forty feet in the quarry parking lot at the University of Hawaii. The flow is a super-rich alkaline basalt, more specifically classed as a melilite nephelinite, therefore, it cannot be considered a typical Hawaiian basalt. A large specimen, about fifty pounds, was removed from the mid-portion of the outcrop at the quarry parking lot. This specimen was oriented before it was taken from its 'in situ' position. Figure 4-1 is a map of the flow, after Stearns (1939).

The specimen was cored with a two-inch diamond coring-bit and sliced into discs with a rock saw. Each sliced surface was ground and polished parallel to its opposite surface. The cores were taken at three mutually perpendicular orientations. One orientation was taken in the direction of the flow, another normal to the flow layer, and the third was normal to the flow and parallel to the layering. Figure 4-2 is a schematic diagram illustrating the selection of the cores with respect to the rock formation. Two discs were obtained for each orienta-

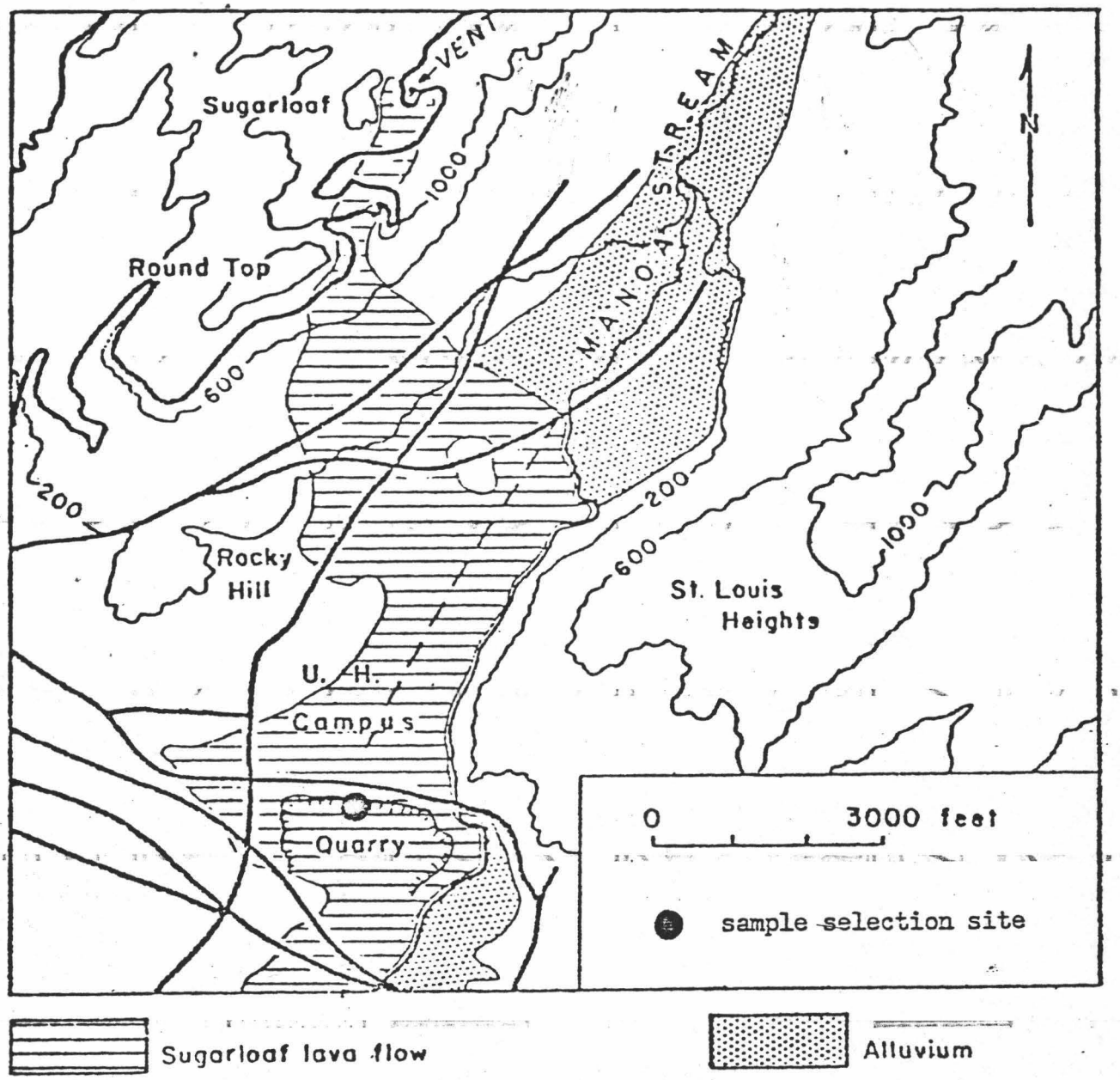

Figure 4-1. Simplified geologic map of Manoa Valley and surroundings, showing the lava flow from Sugarloaf, after Stearns (1939).

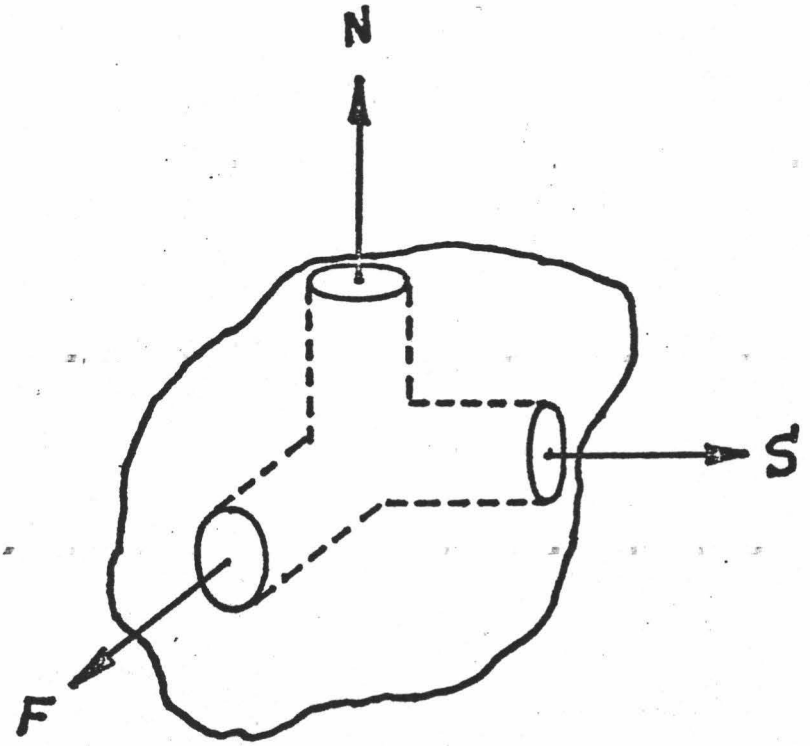

Figure 4-2. Orientation of the rock specimen removed from the Sugarloaf flow at the quarry parking lot of the University of Hawaii. F represents the direction of the flow, S12°W, and S is the strike, N78°W, of the flow layer at the quarry parking lot. N is the normal to the FS-plane.

tion, see Figures 4-3 to 4-5. The discs marked with F are oriented in the direction of the flow, an N indicates the ones normal to the layer and an S identifies the ones parallel to the strike of the layer. Both the F and S specimens are parallel to the layering. The Roman numerals I to VI are relative indicators of the increasing thickness of the samples. The range extends from 0.879 cm for I F to 2.283 cm for VI N.

The upper and lower limits of the thermal conductivity of rocks with low porosity can be estimated by a method described by Birch and Clark (1940), if the constituent minerals and the thermal conductivities of these minerals are known. The equation for the bulk thermal conductivity of a physical model with the mineral grains arranged in a parallel orientation to the direction of heat flow is

$$k_p = v_1k_1 + v_2k_2 + \ldots + v_nk_n \qquad (4.1)$$

where k_p is the upper limit of the thermal conductivity, $v_1,v_2,\ldots,v_n$ are the fractional volumes of the minerals 1,2,...,n, and $k_1,k_2,\ldots,k_n$ are the thermal conductivities of the minerals 1,2,...,n. The equation for the thermal conductivity, k_s, where the mineral grains are arranged in a layered sequence with respect to the direction of heat flow, is given by

$$1/k_s = v_1/k_1 + v_2/k_2 + \ldots + v_n/k_n. \qquad (4.2)$$

This is the lower limit of the thermal conductivity for the rock.

The proportions of minerals comprising the Sugarloaf flow have been analyzed by Winchell (1947). There is a discrepency in the analysis since the proportions of the minerals by volume percentage sum to 113%. An attempt to correct this discrepency is made by dividing the listed proportions by 113 and multiplying the quotient by 100. The

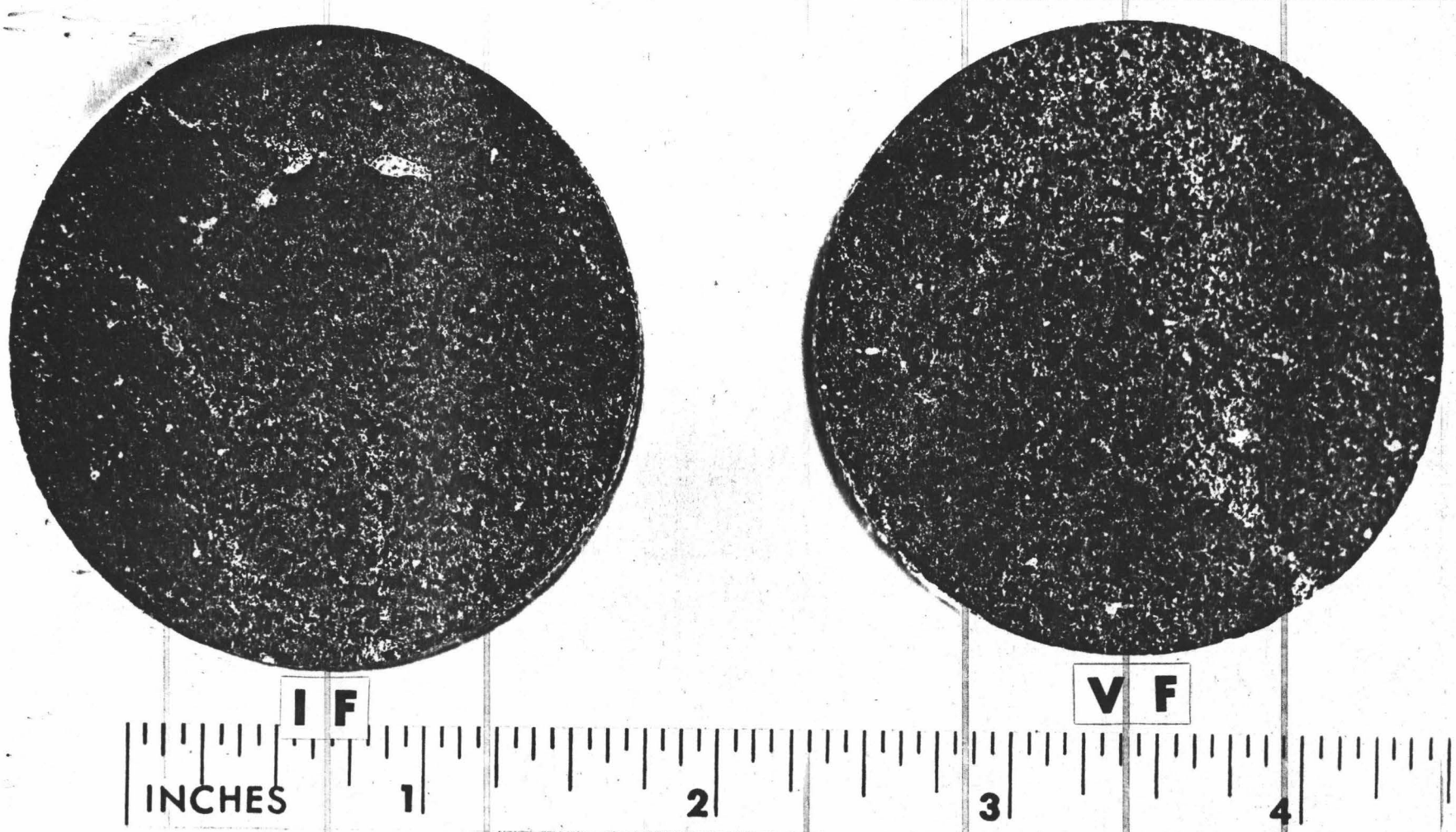

Figure 4-3. Core samples from the Sugarloaf lava flow selected in the direction of the flow.

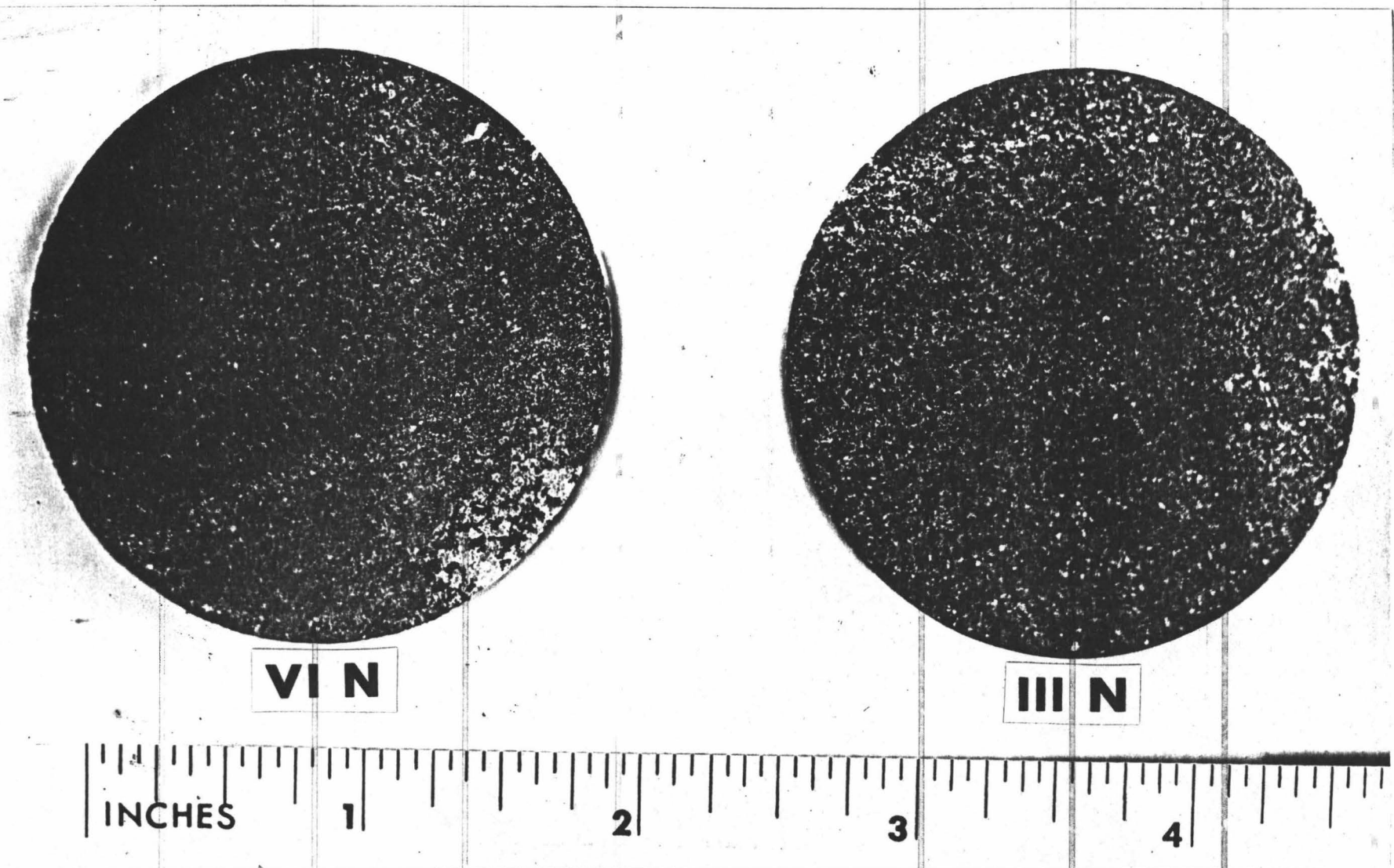

Figure 4-4. Core samples from the Sugarloaf lava flow selected normal to the flow layer.

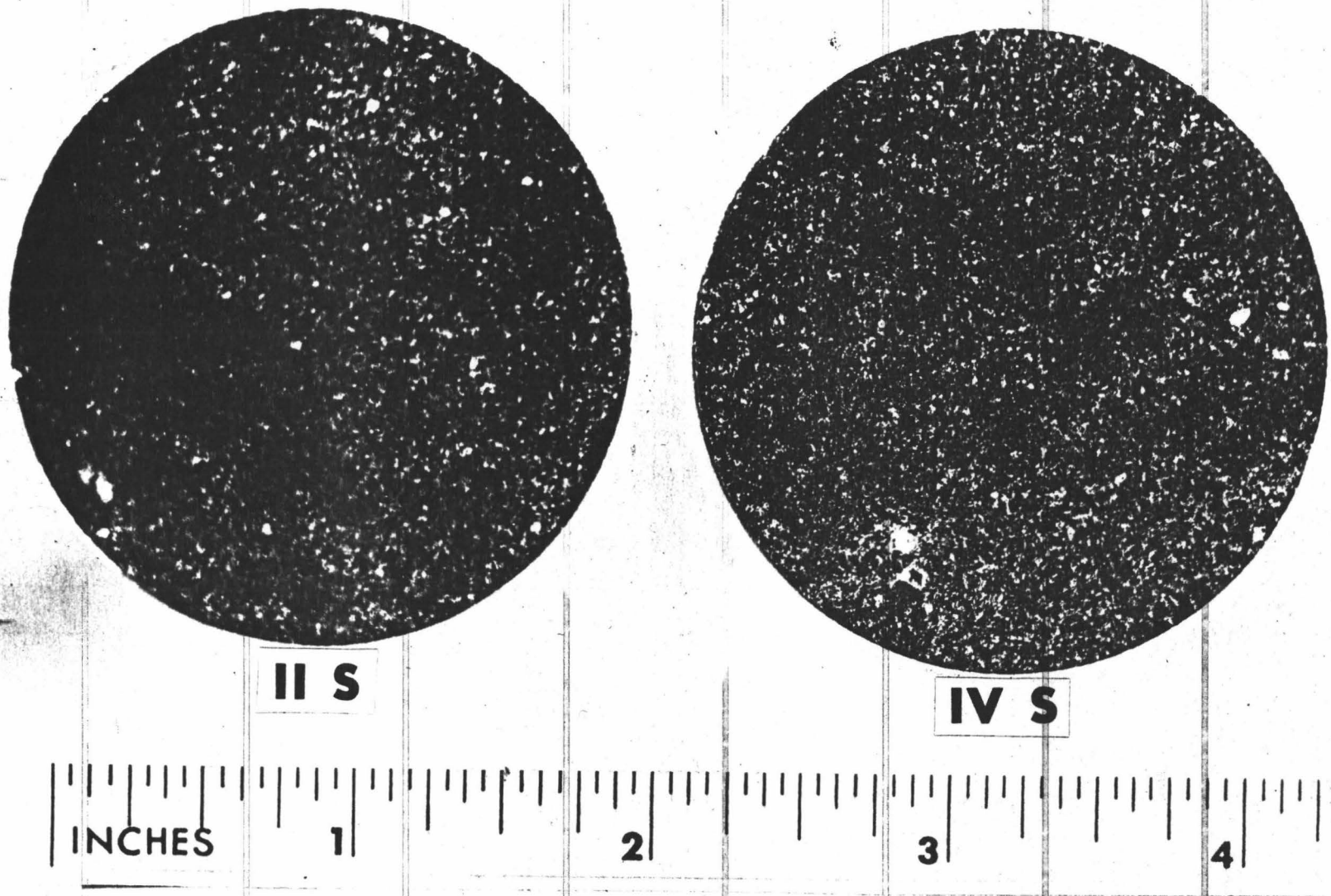

Figure 4-5. Core samples from the Sugarloaf lava flow selected parallel to the strike of the flow layer.

thermal conductivities of rock-forming minerals have been compiled by Horai (1971). Table 4-1 is a summary of these studies, as computed for the Sugarloaf flow. If we use equations (4.1) and (4.2) to define the upper and lower limits of the thermal conductivity for the Sugarloaf flow, we find k_p = 0.00624 cal/sec cm °C and k_s = 0.00525 cal/sec cm °C.

In this study the anisotropy of the thermal conductivity for the Sugarloaf flow is examined for two possible anisotropic cases. The first case is with the thermal conductivity different in three mutually perpendicular directions. Equations (2.6) describe the heat flux of the medium in this anisotropic form. The second case is with the thermal conductivity of orientations parallel to the layering are equal, but different from the thermal conductivity of the orientation normal to the layering. This is called transverse anisotropy and is represented by equations (2.7).

Each sample disc was measured independently ten times with the method described in Chapter 3. These measurements along with the regression equations, standard errors of estimate and reproducibility errors are listed in Tables 4-2 through 4-7. Figure 4-6 is a composite plot of these regression lines in the temperature range 25-50°C.

Two features of these measurements are notable. The regression lines tend to fall into two groups, one for the N samples and the other including both the S and F samples. The temperature coefficients for these regression lines are all less than 1% of the thermal conductivity value. If we consider the small population of measurements, only ten for each sample, and the large standard errors of estimate, about 2.5 times greater than that for the fused quartz measurements, then these

Table 4-1. Thermal conductivities and proportions of minerals in the Sugarloaf flow.

Mineral Name	Content (vol %)	Corrected (vol %)	Thermal Conductivity (cal/sec cm °C)
Augite	5	4.4	0.00913
Olivine	15	13.3	0.01092
Melilite	30	26.5	0.00366
Ores:	2	1.8	
Magnetite		1.08	0.01218
Ilmenite		0.72	0.00567
Pyroxene	25	22.1	0.01050
Nepheline	35	31.0	0.00413
Analcime	1	0.9	0.00303
	113	100.00	

Table 4-2. Thermal-conductivity measurements of the Sugarloaf flow, sample number I F.

Date	Time of Day	Ambient Air Temperature (°C)	Sample Mean Temperature (°C)	Thermal Conductivity (cal/sec cm °C)
16Jun74	----	----	41.35	0.0036
29Jun74	----	----	37.13	0.0035
31Jan75	2100	24.6	43.42	0.0036
1Feb75	1500	25.7	43.78	0.0037
1Feb75	2300	25.9	41.19	0.0039
2Feb75	0815	24.5	39.07	0.0041
2Feb75	1340	26.3	28.74	0.0038
9Feb75	0835	22.7	20.90	0.0038
9Feb75	1105	24.4	21.36	0.0040
9Feb75	1340	26.3	21.69	0.0040

Regression equation: $k = 4.2 - 0.011\,T$ mcal/sec cm °C

Standard error of estimate = 0.19 mcal/sec cm °C

Mean reproducibility error = 3.53%

Sample disc thickness = 0.879 cm

Sample surface area = 23.300 cm^2

Table 4-3. Thermal-conductivity measurements of the Sugarloaf flow, sample number II S.

Date	Time of Day	Ambient Air Temperature (°C)	Sample Mean Temperature (°C)	Thermal Conductivity (cal/sec cm °C)
16Jun74	----	----	36.09	0.0033
26Jun74	----	----	34.64	0.0034
29Jun74	----	----	44.70	0.0037
9Feb75	1515	27.3	38.36	0.0036
9Feb75	1830	26.3	39.08	0.0035
14Feb75	1940	25.5	40.44	0.0034
15Feb75	0730	23.1	39.44	0.0035
15Feb75	1335	27.3	26.58	0.0034
15Feb75	1535	28.0	23.89	0.0033
15Feb75	1845	28.7	24.87	0.0035

Regression equation: $k = 3.1 + 0.012\ T$ mcal/sec cm °C

Standard error of estimate = 0.13 mcal/sec cm °C

Mean reproducibility error = 2.61%

Sample disc thickness = 1.127 cm

Sample surface area = 23.072 cm^2

Table 4-4. Thermal-conductivity measurements of the Sugarloaf flow, sample number III N.

Date	Time of Day	Ambient Air Temperature (°C)	Sample Mean Temperature (°C)	Thermal Conductivity (cal/sec cm °C)
1Mar75	1155	24.7	39.74	0.0050
1Mar75	1505	26.1	36.60	0.0051
1Mar75	2125	25.1	35.96	0.0052
15Mar75	1705	25.7	39.42	0.0053
15Mar75	2015	25.5	43.11	0.0054
15Mar75	2325	25.0	30.20	0.0051
16Mar75	0825	23.3	32.29	0.0047
16Mar75	1035	23.7	29.43	0.0049
16Mar75	1245	24.6	29.22	0.0047
16Mar75	1715	26.3	28.94	0.0052

Regression equation: $k = 4.2 + 0.025\ T$ mcal/sec cm °C

Standard error of estimate = 0.19 mcal/sec cm °C

Mean reproducibility error = 2.93%

Sample disc thickness = 1.234 cm

Sample surface area = 22.918 cm^2

Table 4-5. Thermal-conductivity measurements of the Sugarloaf flow, sample number IV S.

Date	Time of Day	Ambient Air Temperature (°C)	Sample Mean Temperature (°C)	Thermal Conductivity (cal/sec cm °C)
16Jun74	----	----	42.75	0.0034
23Jun74	----	----	35.52	0.0036
27Jun74	----	----	34.38	0.0035
2Feb75	1600	26.7	45.72	0.0042
2Feb75	1920	27.0	46.15	0.0039
7Feb75	1930	25.0	31.99	0.0037
7Feb75	2220	24.3	30.29	0.0037
8Feb75	0030	23.9	27.89	0.0040
8Feb75	0815	22.3	26.83	0.0039
8Feb75	1815	27.1	39.88	0.0042

Regression equation: $k = 3.6 + 0.006\,T$ mcal/sec cm °C

Standard error of estimate = 0.28 mcal/sec cm °C

Mean reproducibility error = 5.61%

Sample disc thickness = 1.317 cm

Sample surface area = 23.200 cm^2

Table 4-6. Thermal-conductivity measurements of the Sugarloaf flow, sample number V F.

Date	Time of Day	Ambient Air Temperature (°C)	Sample Mean Temperature (°C)	Thermal Conductivity (cal/sec cm °C)
16Jun74	----	----	41.00	0.0040
22Jun74	----	----	35.81	0.0038
28Jun74	----	----	37.07	0.0042
15Feb75	2005	27.1	38.31	0.0040
15Feb75	2320	26.5	37.95	0.0041
16Feb75	0920	24.0	38.99	0.0040
17Feb75	1110	24.9	25.27	0.0039
17Feb75	1310	26.0	23.38	0.0039
17Feb75	1520	26.6	25.03	0.0043
17Feb75	1840	26.6	20.59	0.0042

Regression equation: $k = 4.2 - 0.004\,T$ mcal/sec cm °C

Standard error of estimate = 0.15 mcal/sec cm °C

Mean reproducibility error = 2.88%

Sample disc thickness = 1.331 cm

Sample surface area = 22.590 cm^2

Table 4-7. Thermal-conductivity measurements of the Sugarloaf flow, sample number VI N.

Date	Time of Day	Ambient Air Temperature (°C)	Sample Mean Temperature (°C)	Thermal Conductivity (cal/sec cm °C)
16Jun74	----	----	45.17	0.0046
23Jun74	----	----	43.00	0.0043
28Jun74	----	----	42.52	0.0044
8Mar75	0840	23.5	43.47	0.0051
9Mar75	0650	22.1	43.71	0.0050
14Mar75	1840	24.7	47.10	0.0050
14Mar75	2225	24.9	34.44	0.0047
15Mar75	0900	23.0	34.63	0.0043
15Mar75	1145	25.0	33.11	0.0047
15Mar75	1425	26.1	35.31	0.0048

Regression equation: $k = 3.9 + 0.019\ T$ mcal/sec cm °C

Standard error of estimate = 0.30 mcal/sec cm °C

Mean reproducibility error = 5.28%

Sample disc thickness = 2.341 cm

Sample surface area = 23.115 cm^2

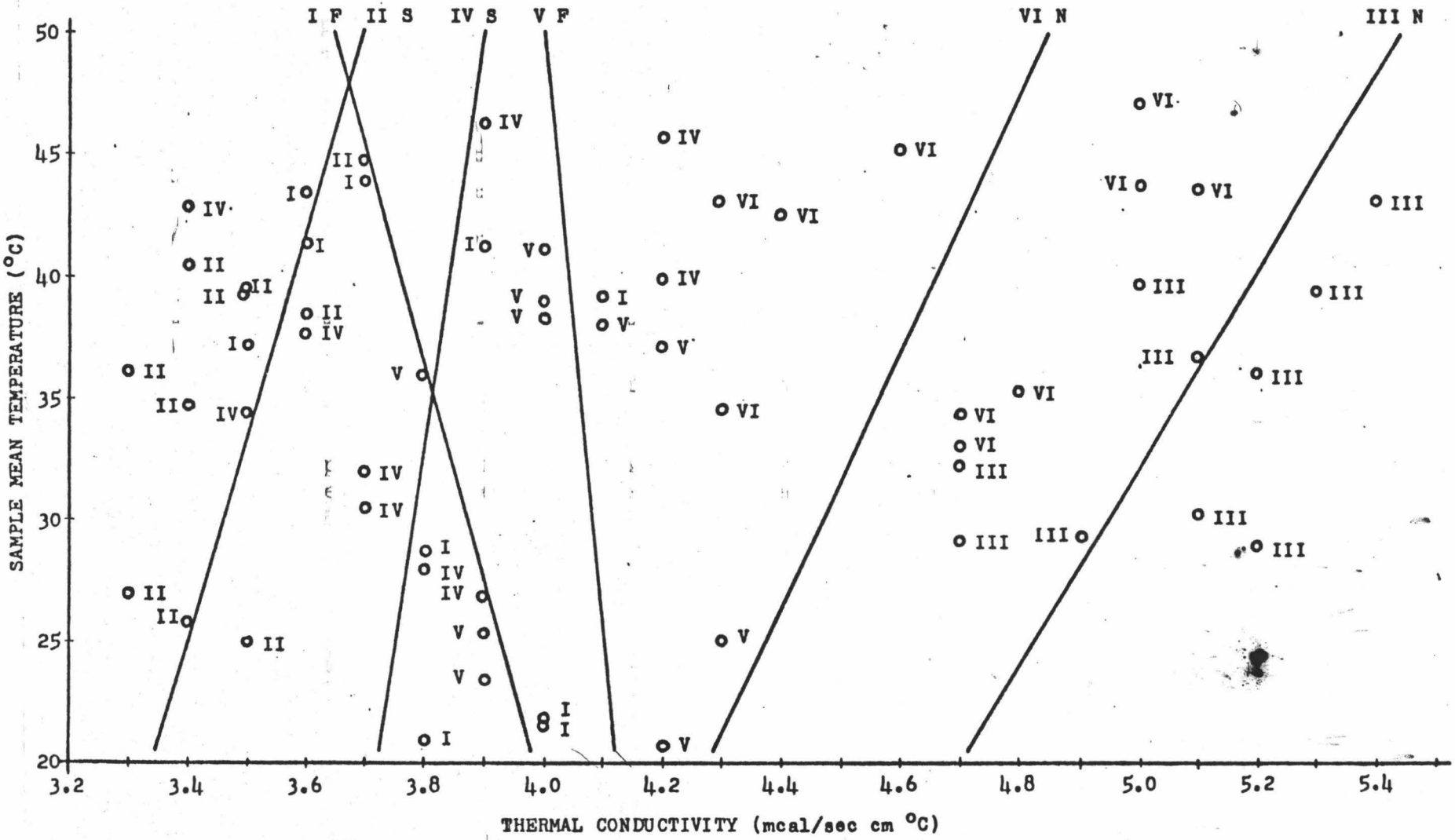

Figure 4-6. Graph of the regression lines from the thermal-conductivity measurements made on samples from the Sugarloaf lava flow.

measurements can be evaluated without temperature dependence. Table 4-8 is a listing of the means and standard deviations of the individual sample discs and different groupings of the sample discs.

All of the measured values are smaller than the value 0.00525 cal/sec cm °C computed, for equation (4.2), to be the lower limit. Two possible explanations for these low values follow. Winchell (1947, p. 21) reported only minor traces of apatite, zeolite and pegmatoid in the Sugarloaf flow. He does state in his summary that the secondary minerals, zeolite chabazite and phillipsite, occur in pegmatoid zones in the Sugarloaf flow where quarries have exposed the interior of the rock. This is the case for the sample obtained for this study. In Figures 4-3 through 4-5 the light colored veins are the pegmatoid and the white phenocrysts are zeolite. These minerals appear to comprise as much as 10% of the surfaces shown in Figure 4-3. The thermal conductivity of chabazite is 0.00292 cal/sec cm °C.

If we assume the mineral composition of the sample obtained contains 10% zeolitic chabazite and 5% less olivine and 5% less pyroxene, the lower limit for the thermal conductivity would then be 0.00464 cal/sec cm °C. This correction only rationalizes the N samples; the others still fall outside the range theoretically possible.

A second explanation for the low measured values is that during the measurements, the glycerin film was observed to be absorbed by the sample discs. The absorbed glycerin appeared to be very shallow in its penetration since the discoloration of the glycerin-wetted discs viewed from the sides under hand lens extended only about an eighth of an inch into the discs from the surfaces. It was possible to dry the glycerin from

Table 4-8. Statistical summary of thermal-conductivity measurements of samples from the Sugarloaf flow.

Sample(s)	Mean Thermal Conductivity (cal/sec cm °C)	Standard Deviation (cal/sec cm °C)
I F	0.0038	0.00021
II S	0.0035	0.00015
III N	0.0051	0.00022
IV S	0.0038	0.00027
V F	0.0040	0.00015
VI N	0.0047	0.00030
I F + V F	0.0039	0.00022
II S + IV S	0.0036	0.00027
III N + VI N	0.0049	0.00032
I F + II S + IV S + V F	0.0038	0.00028

the samples by heating them in an oven. If the glycerin absorption were a shallow phenomenon, it would not cause a thermal short circuit between the copper discs. But the lack of glycerin at the contact surfaces of the copper discs would increase the contact resistance, thus causing the computed value of the thermal conductivity to be less than the true values. This problem has been discussed in greater detail in Chapter 3. A suggested method for overcoming the glycerin absorption problem is set forth in Chapter 8.

The observation of glycerin absorption indicates that the sample discs have at least a small porosity. Robertson and Peck (1974) have measured the thermal conductivity of Hawaiian basalts with varying porosities. They conclude that the difference between observed and calculated thermal conductivities for air-saturated and water-saturated samples is due to the insulating effect of micropores and thin microfractures that formed during the initial cooling of the volcanic samples in the molten state. This effect could also be used to explain, in part, the low values measured in this study. It is also possible that the coring and sample preparation produced microfractures at the surfaces of the specimens.

If we assume the contact resistance is constant in each of the samples measured, then a ratio of anisotropy computed from the apparent thermal-conductivity values would differ from the ratio of the true values by a small amount. The anisotropy ratio is 0.84 for the apparent thermal-conductivity values calculated from equation (3.5) using the values obtained by equations (4.1) and (4.2) and assuming the thermal conductivity across the interface is an order of magnitude smaller, the

thickness of the contact interface is 0.0025 cm, and the sample thickness is 1.0 cm. If we reduce the same thermal-conductivity values by 30% and recompute the apparent thermal conductivities, then the ratio of anisotropy is also 0.84.

In Table 4-8 the thermal conductivity values of the F samples differ from each other by 6.7%, the S samples differ by 9.6% and the N samples by 7.8%. These variations can be attributed, in part, to the variations of the mineral proportions within the rock mass, and in part, to the error in the measurement method. If we group the data to include all the data for a given orientation F, S and N, then the thermal-conductivity values of the F and S data differ by only 7.6%, see Table 4-8. This difference is comparable to the variations found in the samples of a single orientation. Hence, there is no significant anisotropy between the F and S orientations. These orientations are both parallel to the flow layering, and all of the data in these two orientations can be grouped and classed as a parallel orientation. This is a case of transverse anisotropy.

Table 4-8 shows a significant difference of 29% between the measured thermal-conductivity values of the normal and parallel orientations. Kappelmeyer and Haenel (1974, p. 52) define anisotropy of thermal conductivity of rocks as the ratio of the values parallel to the lamination to the values normal to the lamination. The anisotropy for this measurement is 0.78.

A suggested explanation for the existence of this transverse anisotropy of thermal conductivity within the Sugarloaf flow follows. The relative large crystals, compared to the crystals of other basalts,

would indicate the lava layer cooled slowly from its molten state. Also the lava layer is thicker than most, approximately forty feet at the quarry parking lot. The thickness of the layer combined with an extended cooling period would provide conditions favorable to the formation of convection cells within the molten layer. If these thermal convection cells had formed, then the vertical motion would cause the prismatic minerals to align in a vertical direction at certain locations in the layer. And if we further assume the samples measured in this study came from such a location, then transverse anisotropy of thermal conductivity would exist in the measurements.

To test this hypothesis, a thin-section analysis was made on core sample number VI N, with assistance from Daniel Palmiter. One thin-section was taken normal to the flow layer, and two thin-sections were taken parallel to the layering but normal to each other. No preferred alignment of prismatic crystals was observed in any of these sections. This suggests the transverse anisotropy is due to composition rather than structure.

Part II

PERIODIC AND TRANSIENT METHODS FOR DETERMINING THERMAL CONDUCTIVITY IN THE LABORATORY AND THE FIELD

Chapter 5

NONSTEADY-STATE MEASUREMENT OF THERMAL CONDUCTIVITY

In nonsteady-state methods, the temperature distribution in the specimen varies with time. The time rate of temperature change at certain positions along a specimen is measured and no measurement of the heat flow is required. Nonsteady-state methods are used in the laboratory for expedient measurements and are always used for 'in situ' measurements, both in wells and shallow soil-probes. Nonsteady-state methods fall into two major categories, the periodic and the transient heat-flow methods. Methods from both categories were used in this study and each of these methods is described below.

Periodic Heat-Flow Methods.

In periodic heat-flow methods, the heat supplied to the specimen is modulated with a fixed period. The resulting temperature wave, which propagates through the specimen with the same period, is attentuated by absorption as it progresses. The thermal diffusivity of the specimen controls the wavelength of the wave in the specimen. The thermal diffusivity is related to the thermal conductivity through the relation given in Kappelmeyer and Haenel (1974, p. 10) as

$$k = D\rho c \tag{5.1}$$

where k is the thermal conductivity (heat flow per unit time per unit distance per degree of temperature), D is the thermal diffusivity (area per unit time), ρ is the density (mass per unit volume) and c is the specific heat (quantity of heat per unit weight per degree of temperature).

The thermal diffusivity can be determined from measurements of amplitude decrement and/or phase difference of the temperature waves between certain positons of the specimen. The decay with depth of the amplitude of the temperature wave is given by

$$T_2 = T_1 \, e^{-(z_2 - z_1)\sqrt{\pi/DP}} \tag{5.2}$$

where T_1 is the amplitude of the temperature wave in the specimen at depth z_1, T_2 is the attenuated amplitude at depth z_2 in the specimen, P is the period of the temperature wave, and D is the thermal diffusivity of the specimen. The phase shift, ϕ, of the attenuated temperature wave between depths z_1 and z_2 is

$$\phi = (z_2 - z_1)\sqrt{\pi/DP}. \tag{5.3}$$

Figure 5-1 is a graph of a temperature wave at one depth and the attenuated temperature wave at a lower depth.

From equations (5.2) and (5.3) the thermal diffusivity can be expressed as a function of the temperature amplitudes by

$$D = \frac{(z_2 - z_1)^2 \pi/P}{[\ln(T_1) - \ln(T_2)]^2} \tag{5.4}$$

and as a function of phase shift by

$$D = (z_2 - z_1)^2 \pi/P\phi^2. \tag{5.5}$$

This method is discussed in more detail by Kirkham and Powers (1972) and by Kappelmeyer and Haenel (1974, p. 87).

The temperature profile curve (temperature versus depth at a given time) can be obtained by measuring the temperature at several depths within the specimen. If this temperature profile curve is acquired a number of times during the penetration of the temperature wave into the specimen, the measurement of the depth at the crossover point of any two

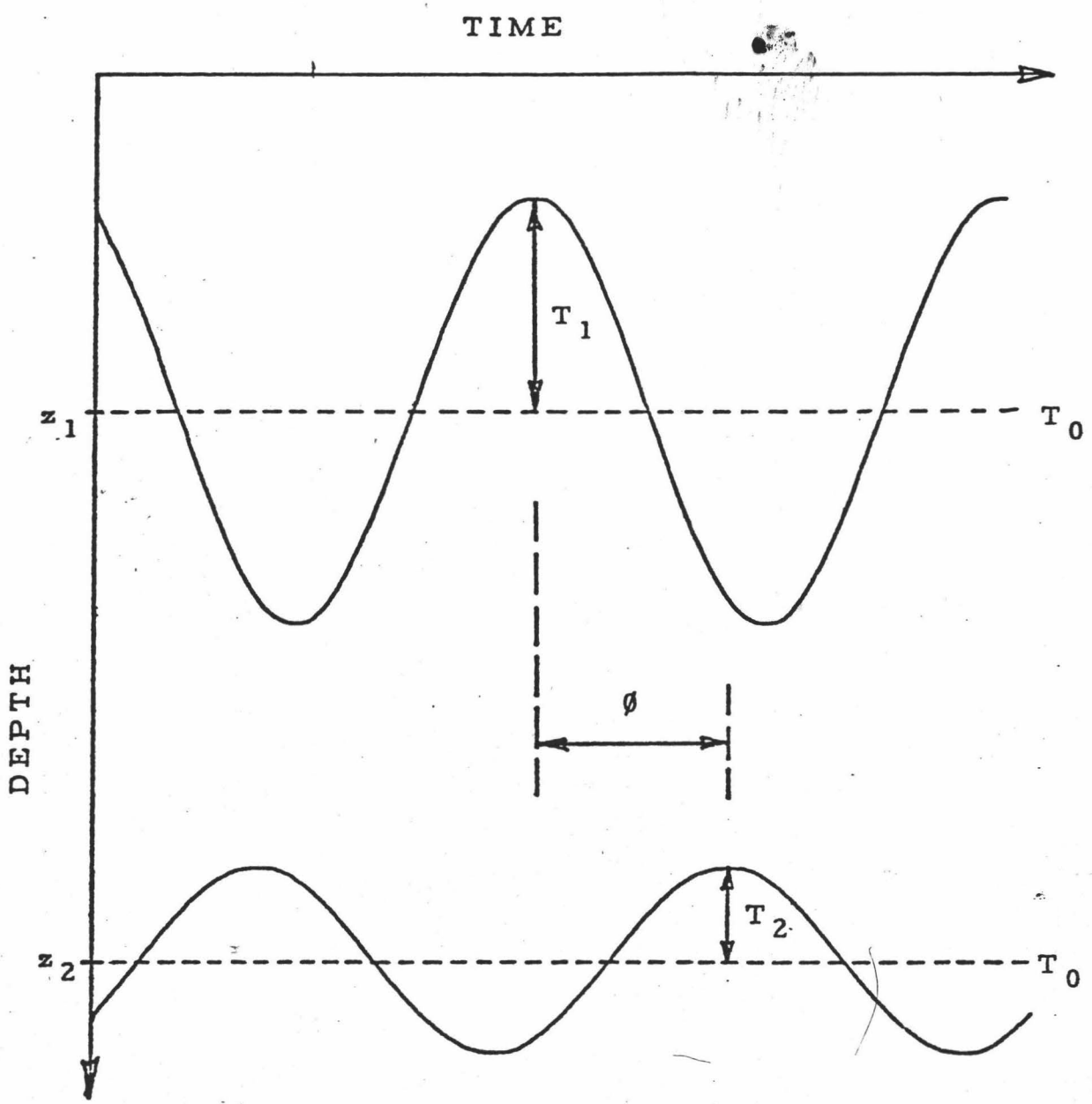

Figure 5-1. Attenuation in the form of amplitude decay and phase lag of a temperature sine wave shown at two positions within the medium.

of the temperature-profile curves within the same periodic cycle provides input data for a method of calculating thermal diffusivity. The relationship provided by Lovering and Goode (1963, p. 27) is *

$$D = \frac{4z_c^2\pi/P}{[(t_1 + t_2)2\pi/P \mp (2n + 1)\pi]^2} \qquad (5.6)$$

where t_1 and t_2 are the times, in seconds, the measurements were taken from the beginning of the driving function, z_c is the depth at the crossover of these two curves, and n is 0, 1, 2, etc., representing the corresponding first, second, third, etc. crossover of the two curves. The thermal diffusivity, D, is the average thermal-diffusivity value of the test material between the crossing points and the level providing the driving function. Figure 5-2 is a graph of two temperature-profile curves measured at separate times within the same periodic cycle.

These periodic methods have been described above as though they were for laboratory-sized specimens. These methods are quite useful for 'in situ' measurements of thermal diffusivity in soil probes and in bore holes less than twenty meters in depth. The annual temperature wave is assumed to be the periodic driving function that propagates the heat through the soil and rock. The thermal conductivity can be indirectly obtained from thermal diffusivity measurements, determined from periodic methods, by either measuring or estimating the density and the specific heat of the test material, thus introducing more measurement error into the thermal-conductivity determination.

---

* The minus-plus was erroneously given as plus-minus.

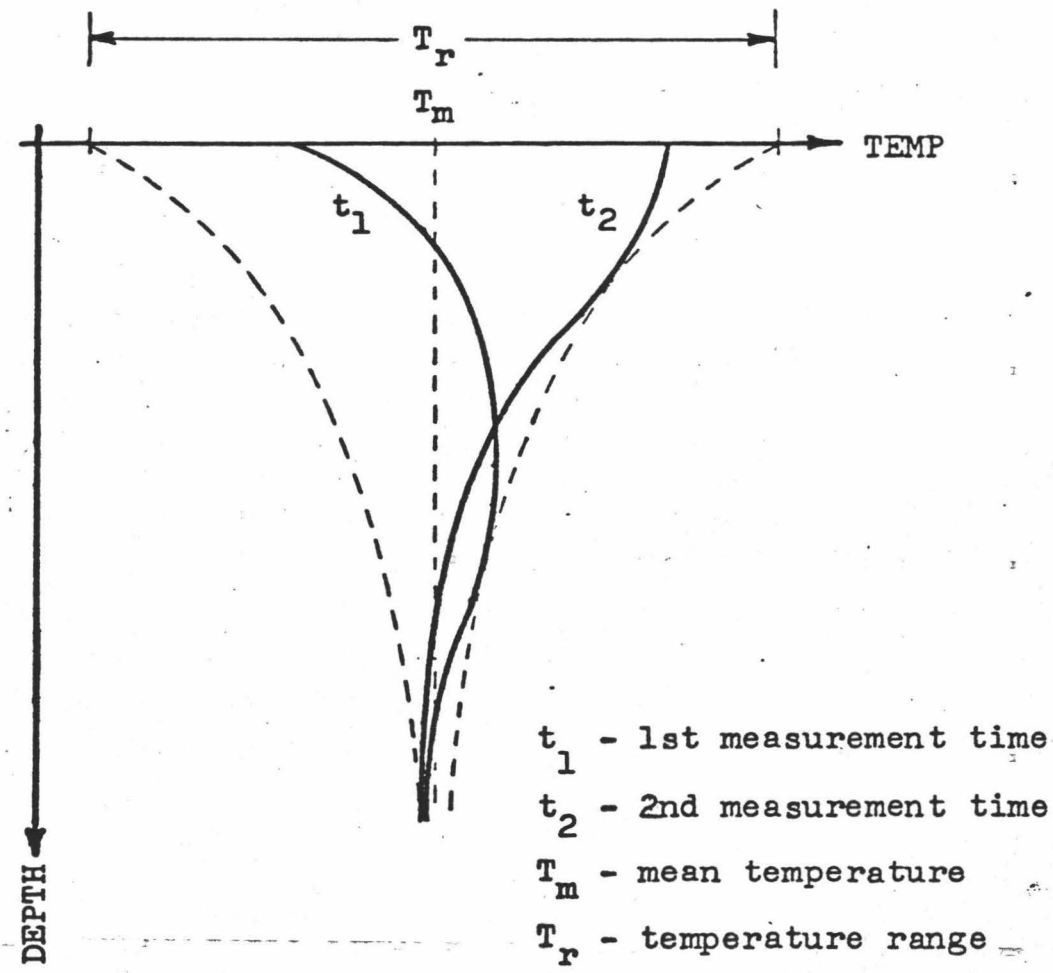

Figure 5-2. Temperature-depth graph depicting the change in position of the temperature profile at two separate times.

Transient Heat-Flow Methods.

The transient heat-flow method used in this study is referred to as a needle-probe technique, and it is used solely for laboratory measurements. In this method a long heater wire, with a diameter less than 1/30 of its length, which serves as a line heat-source, is embedded into a specimen. The heater is then turned on, which produces constant heat, L, per unit length per unit time, and the temperature at the midpoint of the wire is recorded as a function of time. The thermal conductivity is given by the expression

$$k = \frac{L[\ln(t_2/t_1)]}{4\pi(T_2 - T_1)}, \qquad (5.7)$$

where $(T_2 - T_1)$ is the temperature difference at the times t_1 and t_2, after Von Herzen and Maxwell (1959).

The needle probe consists of a hypodermic needle which is soldered to a plug housing. A Rh-Pt heating wire runs the length of the needle and a thermistor is located midway along the length of the needle. A wheatstone bridge and a strip-chart recorder are used to measure the resistance of the thermistor, and a regulated-DC power-supply is used to provide power to the heating wire. Figure 5-3 is a schematic diagram of a needle-probe apparatus.

Conductivity probe #16 was used from the Hawaii Institute of Geophysics heat-flow laboratory. Approximately twenty temperature measurements are recorded at 10-sec time intervals. A regression curve, an exponential, is then fitted to the time-temperature curve, and the thermal conductivity is calculated from equation (5.7). Figure 5-4 is a typical

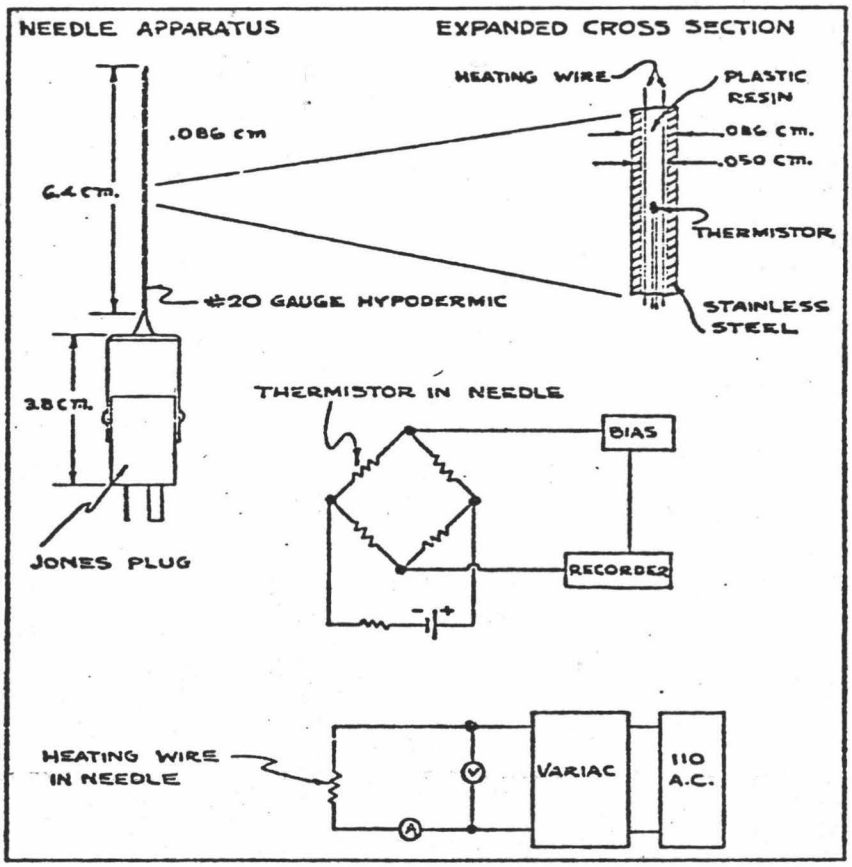

Figure 5-3. Needle-probe apparatus for measuring thermal conductivity, after Von Herzen and Maxwell (1959).

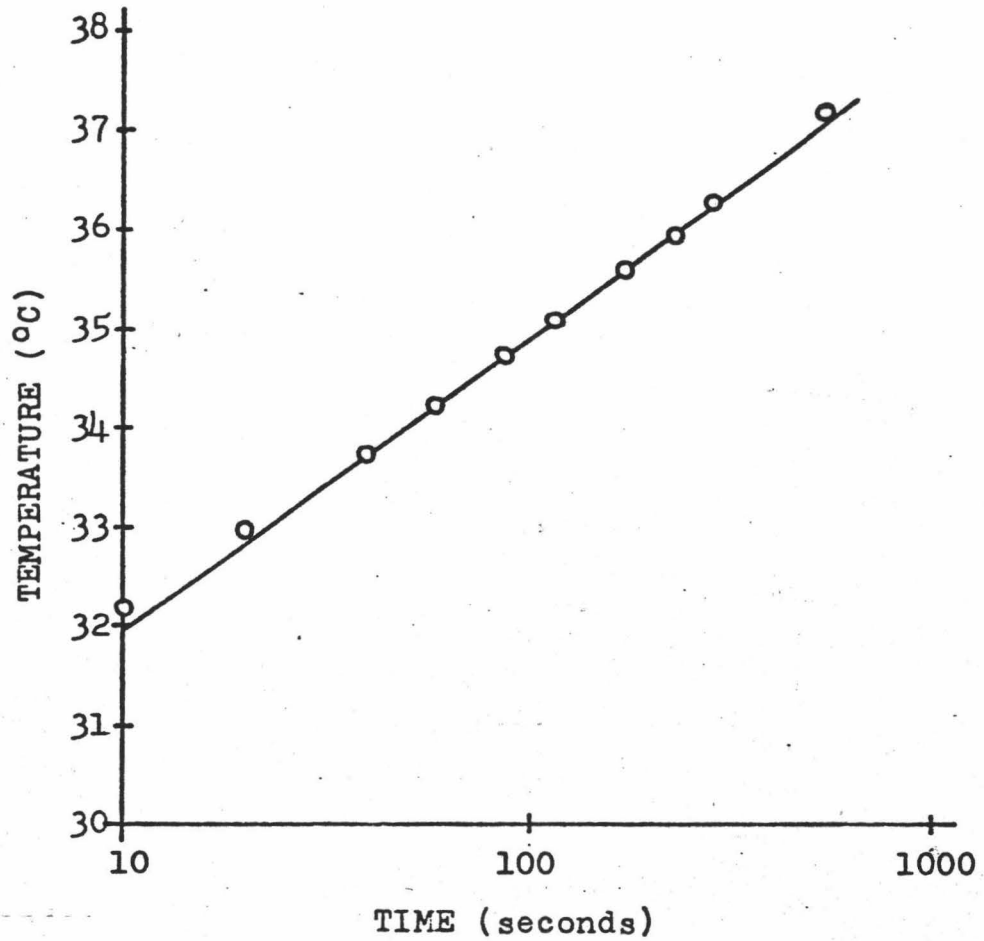

Figure 5-4. Temperature versus time for a needle-probe measurement, after Von Herzen and Maxwell (1959).

log-time versus temperature graph for a needle-probe measurement of a marine sediment.

A limitation of the method is the fact that the thermal conductivity of many earth materials has a small positive temperature dependence; this would increase the thermal-conductivity values by one or two percent near the needle, and by lesser amounts at greater distances from the needle.

Chapter 6

ESTIMATION OF THERMAL DIFFUSIVITY FROM FIELD OBSERVATIONS

Lake Waiau is situated in the Waiau cone which is near the summit of the inactive volcano, Mauna Kea on the island of Hawaii. A more specific location is shown in Figure 6-1. The existence of a negative thermal gradient under Lake Waiau has been determined by Woodcock and Groves (1969). The cause of the anomalous gradient remains uncertain. The answer is contingent on knowledge of the differences in the relative thermal-properties of the lake water, the lake sediment, and the cinders and lava surrounding the lake as well as the thermal regime established in the area by natural processes. The purpose of this study is to determine the thermal conductivity of the lake sediments in which the negative thermal-gradient occurs. This will also allow us to obtain an estimate of the heat flux through the sediments.

Woodcock, et al. (1966) have described the upper two meters of the sediments. This section contains two coarse layers of black ash and several layers of finer gray ash comprising about 5% and 10%, respectively, of the section. The remaining 85% of the sediments are colorful shades of red and olive-green. These colorful layers consist primarily of very fine particles, less than 0.05 mm in diameter, believed to be windblown from local sources, and about 5% is combustible organic materials.

Table 6-1 lists the thermal-probe data obtained by A.H. Woodcock that was used in the thermal-gradient determination. These data have also been used in this study to make estimates of the thermal diffusivity using the nonsteady-state periodic methods described in Chapter 5.

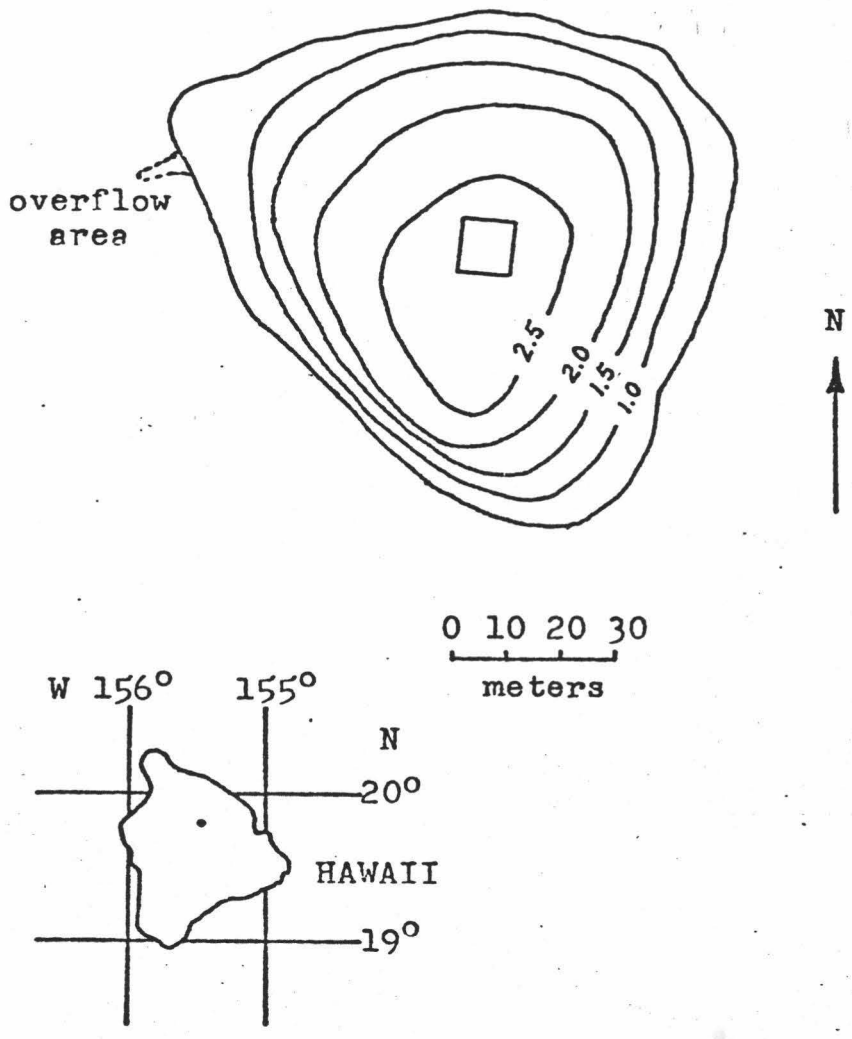

Figure 6-1. Map of Lake Waiau showing estimated depth contours in meters. The inner square marks the limits of the area in which the temperature measurements were made, after Woodcock and Groves (1969).

Depth* (m)	July 7, 1965	July 27	Aug. 17	Aug. 29	Sept. 14	Nov. 9	Jan. 6, 1966	Feb. 15	Mar. 19	May 1	June 1	July 2	July 27	Nov. 1	Dec. 1	Dec. 28	Jan. 26, 1967	Mar. 3	Apr. 8	May 4	July 25
3·0	8·9 ± 0·1	9·2 ± 0·3	8·8 ± 0·2	9·3 ± 0·3	9·6 ± 0·3	7·2 ± 0·1	3·3 ± 0·1	3·4 ± 0·05	5·3 ± 0·15	6·2 ± 0·1	9·0 ± 0·15	9·0 ± 0·25	7·8 ± 0·1	6·4 ± 0·05	6·3 ± 0·2	3·8 ± 0·2	3·5 ± 0·05	5·3 ± 0·05	6·1 ± 0·1	8·0 ± 0·4	8·7 ± 0·1
3·5	8·4 ± 0·15	8·2 ± 0·2	8·1 ± 0·15	8·0 ± 0·15	8·3 ± 0·2	7·4 ± 0·1	4·2 ± 0·2	4·0 ± 0·2	4·8 ± 0·05	5·9 ± 0·05	8·0 ± 0·25	7·1 ± 0·1	7·7 ±0·1	7·1 ± 0·2	7·0 ± 0·05	5·1 ± 0·2	3·7 ± 0·15	4·8 ± 0·1	5·9 ± 0·1	6·5 ± 0·3	7·9 ± 0·2
4·0	7·6 ± 0·15	7·3 ± 0·2	7·5 ± 0·15	7·4 ± 0·1	7·4 ± 0·15	7·6 ± 0·05	5·2 ± 0·2	5·1 ±0·2	4·9 ± 0·05	5·8 ± 0·05	6·7 ± 0·2	6·8 ± 0·05	7·3 ± 0·1	7·5 ± 0·05	7·1 ± 0·05	6·3 ± 0·2	4·7 ± 0·2	4·9 ± 0·1	5·8 ± 0·05	5·9 ± 0·1	7·3 ± 0·05
4·5	7·0 ± 0·1	6·8 ± 0·1	7·0 ± 0·1	7·0 ± 0·1	6·8 ± 0·1	7·3 ± 0·1	6·1 ± 0·2	5·6 ± 0·1	5·0 ± 0·05	5·9 ±0·05	6·0 ± 0·1	6·5 ± 0·05	6·7 ± 0·05	7·2 ± 0·1	7·2 ± 0·05	6·8 ± 0·1	5·6 ± 0·15	5·4 ± 0·1	5·8 ± 0·05	5·9 ± 0·1	6·95 ± 0·05
5·0	6·7 ± 0·05	6·8 ± 0·1	6·7 ± 0·1	6·7 ± 0·05	6·6 ± 0·05	7·0 ± 0·05	6·8 ± 0·1	6·0 ± 0·05	5·4 ± 0·05	6·0 ± 0·05	5·9 ± 0·05	6·3 ± 0·05	6·4 ± 0·05	7·0 ± 0·05	7·1 ± 0·05	6·9 ± 0·05	6·1 ± 0·05	5·8 ± 0·1	6·0 ± 0·05	6·1 ± 0·1	6·6 ± 0·05
6·0	6·3 ± 0·05	6·3 ± 0·05	6·5 ± 0·05	6·35 ± 0·05	6·35 ± 0·05	6·65 ± 0·05	7·0 ± 0·05	6·2 ± 0·05	6·05 ± 0·05	6·2 ± 0·05	6·0 ± 0·05	6·3 ± 0·05	6·2 ± 0·05	6·65 ± 0·05	6·85 ± 0·05	6·9 ± 0·05	6·4 ± 0·05	6·15 ± 0·05	6·3 ± 0·05	6·3 ± 0·05	6·35 ± 0·05
7·0	6·4 ± 0·05	6·3 ± 0·05	6·45 ± 0·05	6·25 ± 0·05	6·25 ± 0·05	6·4 ± 0·05	6·7 ± 0·05	6·15 ± 0·05	6·2 ± 0·05	6·3 ± 0·05	6·1 ± 0·05	6·2 ± 0·05	6·1 ± 0·05	6·3 ± 0·05	6·8 ± 0·05	6·55 ± 0·05	6·2 ± 0·05	6·35 ± 0·05	6·4 ± 0·05	6·3 ± 0·05	6·3 ± 0·05

*Depth below water surface; for depth below sediment surface subtract ~ 2·85 m.

Table 6-1. Temperature (°C) at standard depths in Lake Waiau sediments as a function of time, Woodcock and Groves (1969).

The estimates were first made without any attempt to smooth the data, therefore, large variances are to be expected.

Estimates by Amplitude Decay and Phase Lag.

The methods of estimating the thermal diffusivity by the decay of the amplitude and/or the phase shift of a temperature wave as it propagates through a medium are outlined in Chapter 5 after Kirkham and Powers (1972) and Kappelmeyer and Haenel (1974, p. 87). Figure 6-2 is a temperature-time graph of the thermal-probe measurements from Lake Waiau at the 3-meter and the 5-meter depths below the lake surface. A similarity between Figure 6-2 and Figure 5-1 is evident. The amplitudes T_1 and T_2 from Figure 6-2 are taken as one half of the difference of the maximum and the minimum temperature values in each data set. The amplitude is 2.93°C at the 3-meter level and 0.73°C at 5-meters. If we use the equation for temperature variation,

$$D = \frac{(z_2 - z_1)^2 \pi / P}{[\ln(T_1) - \ln(T_2)]^2}, \qquad (5.4)$$

an estimate of the thermal diffusivity in the sediment layer between 3 and 5 meters below the lake surface is 0.00205 cm^2/sec.

We can also plot the data for the 5-meter level on an exaggerated vertical scale so the curve is about the same size as the curve for the 3-meter plot. Then by placing one curve on the other and sliding it along the time axis until the curves match, we can estimate the phase lag by measuring the time difference between the zero-time axes. The estimated phase shift between these two curves is 60 days. And with the equation based on the phase lag,

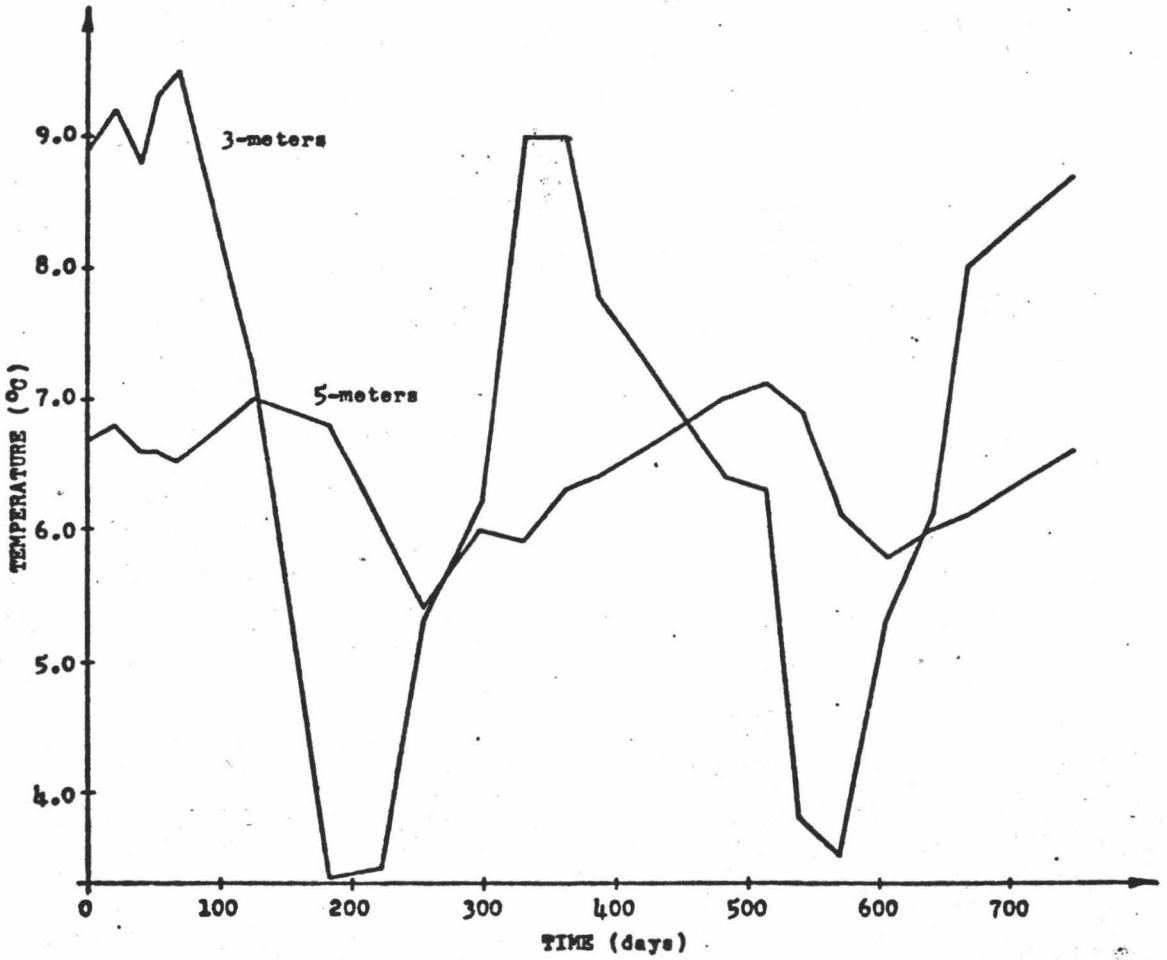

Figure 6-2. Temperature, from thermal probes in Lake Waiau sediment, plotted against time for measurements taken at three and five meters below the water surface.

$$D = (z_2 - z_1)^2 \pi / P\phi^2, \qquad (5.5)$$

we obtain an estimate of 0.00374 cm^2/sec for the thermal diffusivity of the same two-meter layer. There is a difference of 45% between these two methods for this layer of sediments, even though the results are based on the very same set of data.

The data in Table 6-1 has been evaluated for each level of measurements combined with every other level. The results are shown in Table 6-2. The differences between the amplitude estimates and the phase estimates have a mean value of 50%. If we assume that these sediments are isotropic and homogeneous in the layer between the 3-meter and the 7-meter depths, then the thermal diffusivity should be the same for each of the above estimates. The mean thermal-diffusivity value from the amplitude computations is 0.00298 cm^2/sec with a standard deviation of 0.00212, and the mean of the phase computations is 0.00410 cm^2/sec with a standard deviation of 0.0103. The difference between these phase and amplitude estimates is 38%. This difference was attributed to the methodology being inadequate to resolve the unsmoothed data rather than the assumptions, and an alternate methodology was used to try to obtain a more reliable value for the thermal diffusivity.

Estimate by Crossover of Temperature Profiles.

The method of estimating the thermal diffusivity of a medium by the crossover point of two temperature-depth curves (temperature profiles) has been explained in Chapter 5 after work by Lovering and Goode (1963). Figure 6-3 is a graph of the temperature-depth profiles for the measurements made on 27 July 1966 and 28 December 1966 in the sediments of Lake

Table 6-2. Thermal-diffusivity computations from amplitude decay and phase lag of the thermal-probe data taken in Lake Waiau, 1965-1967.

Amplitude Diffusivity (cm^2/sec)	Phase Diffusivity (cm^2/sec)	Upper Depth (cm)	Lower Depth (cm)	Upper Amplitude (°C)	Lower Amplitude (°C)	Phase Lag (days)
0.00284	0.00840	300	350	2.93	2.18	10
0.00175	0.00350	300	400	2.93	1.38	31
0.00204	0.00391	300	450	2.93	1.02	44
0.00205	0.00374	300	500	2.93	0.73	60
0.00264	0.00241	300	600	2.93	0.46	112
0.00307	0.00282	300	700	2.93	0.30	138
0.00118	0.00429	350	400	2.18	1.38	14
0.00176	0.00309	350	450	2.18	1.02	33
0.00186	0.00197	350	500	2.18	0.73	62
0.00260	0.00202	350	600	2.18	0.46	102
0.00311	0.00233	350	700	2.18	0.30	133
0.00289	0.00259	400	450	1.38	1.02	18
0.00243	0.00140	400	500	1.38	0.73	49
0.00336	0.00205	400	600	1.38	0.46	81
0.00387	0.00264	400	700	1.38	0.30	107
0.00208	0.00146	450	500	1.02	0.73	24
0.00355	0.00197	450	600	1.02	0.46	62
0.00412	0.00278	450	700	1.02	0.30	87
0.00495	0.00328	500	600	0.73	0.46	32
0.00512	0.00174	500	700	0.73	0.30	88
0.00529	0.02778	600	700	0.46	0.30	10

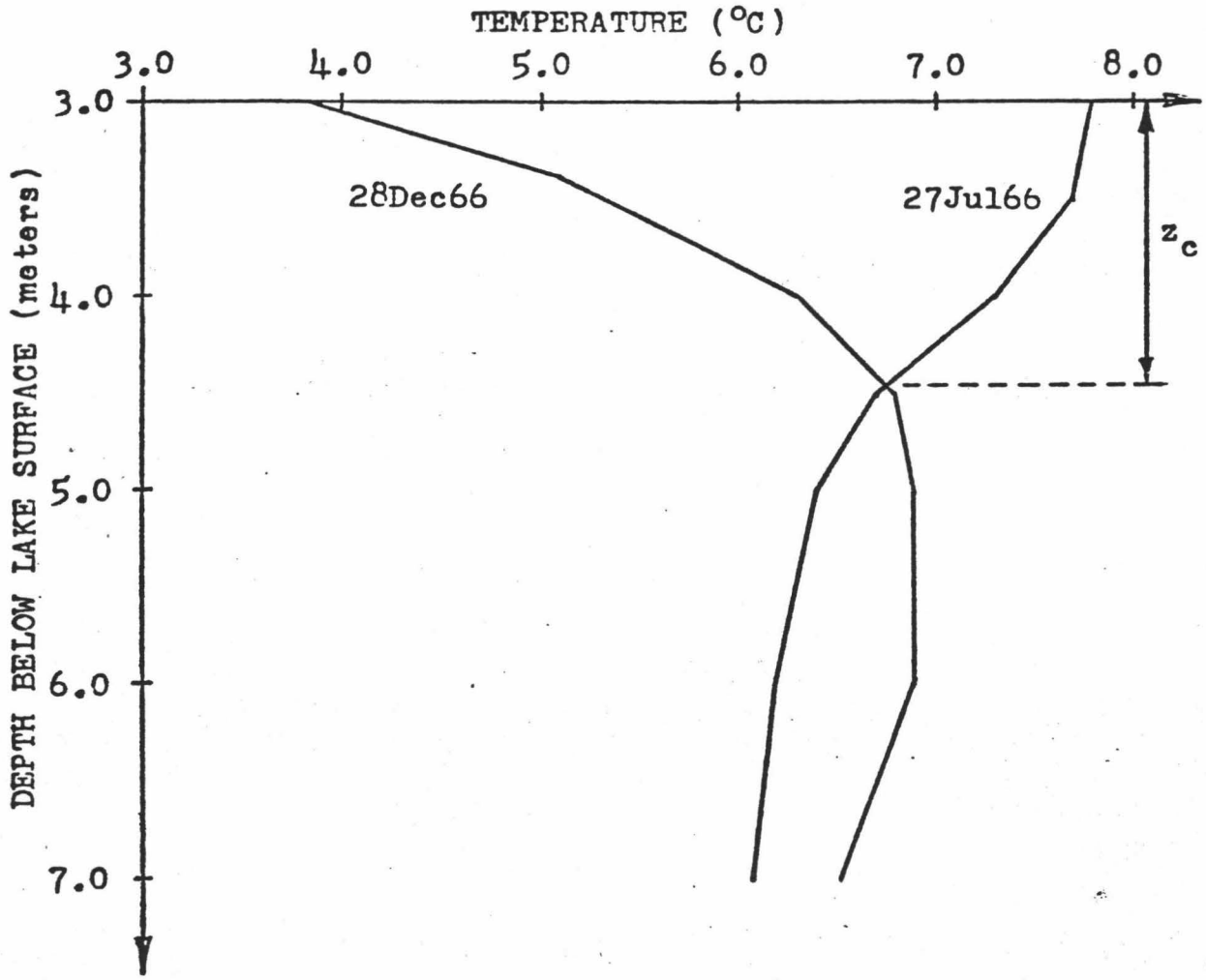

Figure 6-3. Temperature profile of two thermal-probe measurements made in the sediments of Lake Waiau.

Waiau. The crossover depth of these curves occurs at 447 cm. If we assume the temperature wave detected at the 3-meter depth to be the periodic driving function with a period of 365 days, then the thermal diffusivity of the sediments between 300 and 417 cm can be estimated by

$$D = \frac{4z_c^2\pi/P}{[(t_1 + t_2)2\pi/P \mp (2n + 1)\pi]^2} \qquad (5.6)$$

to be 0.0138 cm^2/sec.

Table 6-3 is a listing of 43 pairs of curves evaluated in a similar manner. The mean thermal diffusivity is estimated to be 0.00765 cm^2/sec with a standard deviation of 0.0135, and the distribution was very strongly skewed toward the lower values. The mode of this distribution is 0.00130 cm^2/sec with a standard deviation of 0.00030. The computation is made again under the assumption that the sediment layer between 300 and 682 cm below the lake surface is isotropic and homogeneous. This estimate is about 2-3 times smaller than the estimates using the amplitude decay and phase lag computations.

Such a large difference makes evident that the answer was more dependent upon the method of analysis than on the data. If each method were theoretically correct and used the same data base, then the results should be identical. Each method did seem to have a correct theoretical basis but used different portions of the data, e.g., the temperature amplitudes, the phase difference between depths and only the crossover points. The large difference between the results thus indicated the need to use all of the data available. The following method was suggested by W.M. Adams and was evolved into a practical method with the programming assistance of George Mason.

Table 6-3. Thermal-diffusivity computations from temperature-profile crossings of thermal probes in Lake Waiau.

Thermal Diffusivity (cm^2/sec)	Crossover Depth (cm)	1st Time (days)	2nd Time (days)	Summer Cycle (days)	Intersecting Pair of Measurements
0.00110	317	247	287	366	6Jan66-15Feb66
0.00115	337	181	366	365	1Nov66-4May67
0.00099	339	211	366	365	1Dec66-4May67
0.00122	342	238	303	365	28Dec66-3Mar67
0.00085	343	189	425	366	9Nov65-2Jul66
0.04982	350	59	181	365	2Jul66-1Nov66
0.02314	363	59	211	365	2Jul66-1Dec66
0.00116	371	189	394	366	9Nov65-1Jun66
0.00091	375	189	450	366	9Nov65-27Jul66
0.00125	381	238	339	365	28Dec66-8Apr67
0.00134	383	247	320	366	6Jan66-19Mar66
0.06573	384	105	133	366	17Aug65-14Sep65
0.02493	387	84	189	366	27Jul65-9Nov65
0.02959	387	84	181	365	27Jul66-1Nov66
0.00114	390	287	320	366	15Feb66-19Mar66
0.00115	390	238	366	365	28Dec66-4May67
0.01067	391	133	189	366	14Sep65-9Nov65
0.00104	391	181	447	365	1Nov66-25Jul67
0.01699	394	105	189	366	17Aug65-9Nov65
0.01830	415	84	211	365	27Jul66-1Dec66
0.00106	423	211	447	365	1Dec66-25Jul67
0.00162	425	267	303	365	26Jan67-3Mar67
0.00142	437	247	362	366	6Jan66-1May66
0.01381	447	84	238	365	27Jul66-28Dec66
0.00129	448	247	394	366	6Jan66-1Jul66
0.00620	450	181	211	365	1Nov66-1Dec66
0.00116	466	238	447	365	28Dec66-25Jul67
0.00113	471	247	450	366	6Jan66-27Jul66
0.00126	473	247	425	366	6Jan66-2Jul66
0.00093	475	362	394	366	1May66-1Jul66
0.00176	484	267	339	365	26Jan67-8Apr67
0.00834	490	133	247	366	14Sep65-6Jan66
0.00114	490	267	447	365	26Jan67-25Jul67
0.01161	496	105	247	366	17Aug65-6Jan66
0.00155	500	287	362	366	15Feb66-1May66
0.00166	500	267	366	365	26Jan67-4May67
0.00675	530	181	238	365	1Nov66-28Dec66
0.00594	531	189	247	366	9Nov65-6Jan66
0.00177	600	339	366	365	8Apr67-4May67
0.00123	600	362	450	366	1May66-27Jul66
0.00148	633	339	447	365	8Apr67-25Jul67
0.00156	650	362	425	366	1May66-2Jul66
0.00194	682	303	447	365	3Mar67-25Jul67

Estimate by Improved Method.

Figure 6-4 is a map of the temperature-probe measurements on the time-depth plane. Two distinct features are expressed in the character of the isotherms. The sloping of the troughs and ridges from the left at the top toward the right at the bottom is an indication of the phase lag throughout the layer. And the isotherm gradient decreases markedly from the top to the bottom indicating the decay of the temperature fluctuation with depth in the layer. Thus, the isotherm map is a more continuous and total representation of the propagation of the annual temperature wave through the sediment layer over the time span of the measurement than any two selected depth or time sections through this map.

The temperature, T, at any point in the sediment layer can be represented by the following relation from Lovering and Goode (1963)

$$T = T_m + T_r\, e^{-z\sqrt{\pi/DP}}\, \sin[(t + \phi)2\pi/P - z\sqrt{\pi/DP}\,] \qquad (6.1)$$

where

T_r - temperature range of driving level,

T_m - mean temperature of sediments,

D - thermal diffusivity of sediment layer,

z - depth of temperature measurement,

t - time of temperature measurement, and

ϕ - phase displacement in time.

This equation is then used as a model to obtain a least squares fit of the observed data in Table 6-1, as represented by the isothermal map in Figure 6-4, to various idealized data sets.

The temperature, T, the depth, z, and the time, t, are taken to be

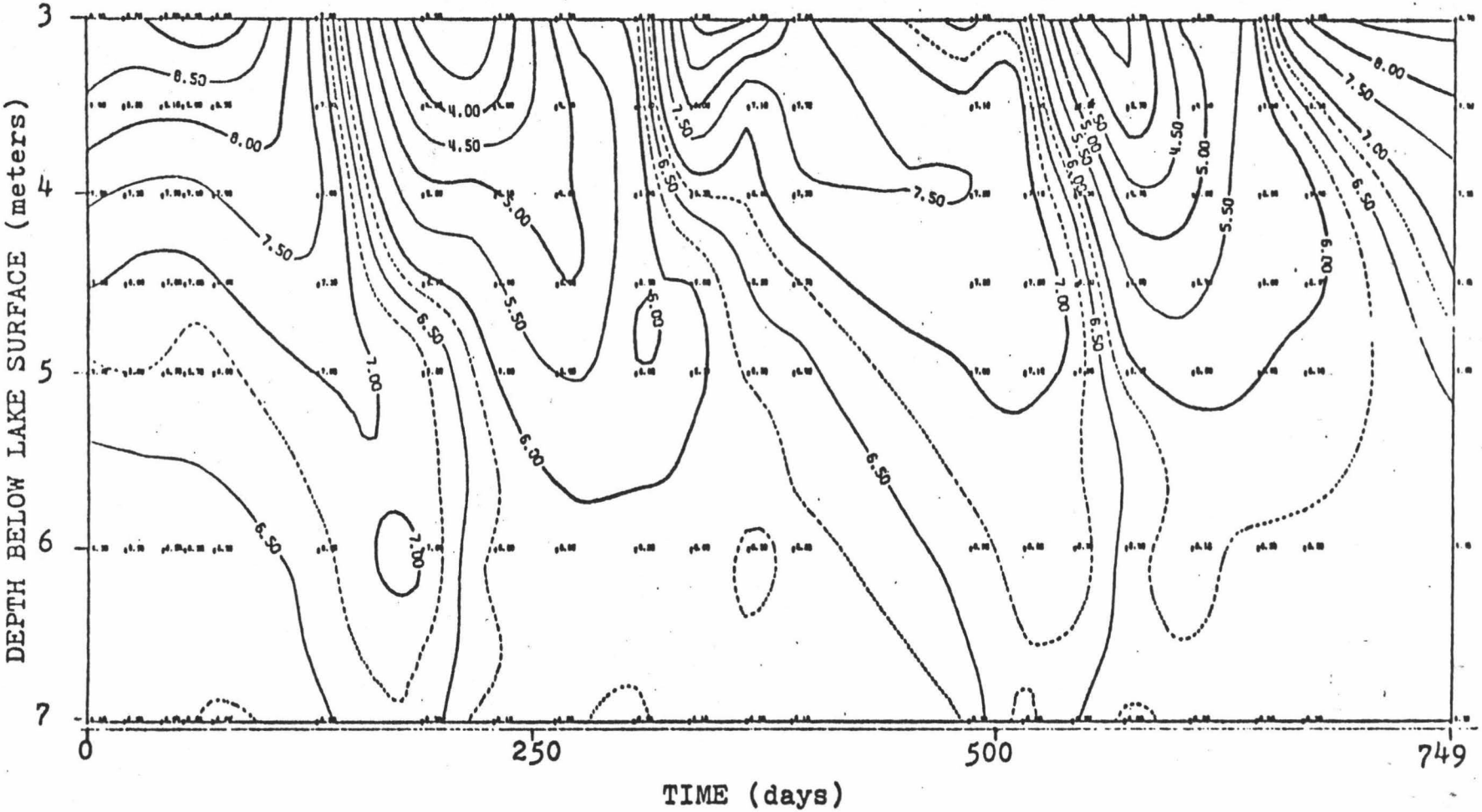

Figure 6-4. Map of isotherms as a function of depth and time from temperature probe data taken in Lake Waiau, after Woodcock and Groves (1969).

the known parameters in this model. The period, P, is set to 365 days and the mean temperature, T_m, is set to 6.3°C from values obtained in previous calculations. This leaves three parameters, the temperature range, T_r, the phase displacement, ϕ, and the thermal diffusivity, D, to be fitted in the estimation.

A well-defined trough on the right side of the map in Figure 6-4 shows a phase shift of 94 days in the four-meter layer. The thermal diffusivity is estimated to be 0.00609 cm^2/sec using the phase lag computation. However, this particular phase lag is not representative of the entire map, and there is no other well-defined ridge or trough that would be a more representative phase lag. If we look at the amplitude decay of the temperature range with depth, the computations give an approximate thermal-diffusivity value of 0.0023 cm^2/sec throughout the sediment layer. Another isotherm map, similar to Figure 6-4, was constructed for the idealized case of a constant thermal diffusivity of 0.0023 cm^2/sec.

The program for calculating least squares was checked and debugged using an artificial data set. Values at the points T(t,z) of the observed data in Figure 6-4 were taken from the idealized map with D = 0.0023 cm^2/sec by superimposing the two maps. When the least squares program was run on the artificial data set, it converged on the expected values of the input parameters, including D = 0.0023 cm^2/sec.

After the general region of the least squares minimum was determined, it was possible to determine the extremum value for the sum of the squared differences between the observed and the idealized data sets by varying the values of the input parameters, T_r, ϕ and D, by small

amounts. The minimum value for the sum of the squares was found to be 30.3462 $(°C)^2$ for 147 data points. The corresponding parameters at this minimum are T_r = 2.655°C, ϕ = 70.67 days and D = 0.00212 cm^2/sec. This calculation then represents the fit of the best regression surface of temperature to the observed temperature surface on the same time-depth plane. An idealized map of the temperature over the same time interval and layer thickness was constructed using these parameters, including D = 0.00212 cm^2/sec, shown in Figure 6-5. A copy of the computer program used in this estimate is listed in the appendix.

Heat flux requires knowledge of the thermal gradient and the thermal conductivity. The thermal gradient has been determined by Woodcock and Groves (1969). It is now necessary to convert the thermal-diffusivity estimate from above to a thermal-conductivity value. This is accomplished in the next chapter along with direct thermal-conductivity measurements of the sediments with the steady-state apparatus.

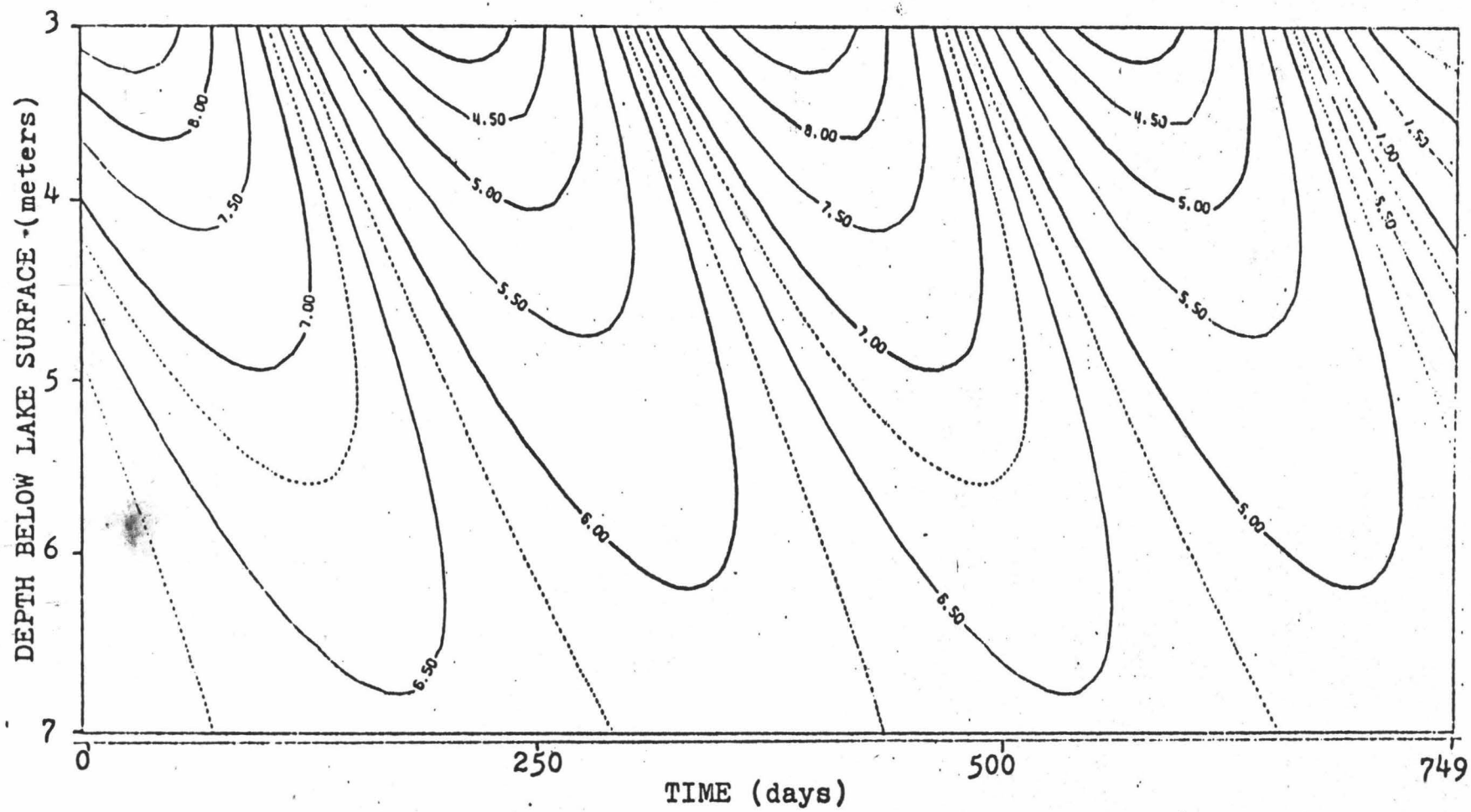

Figure 6-5. Map of isotherms as a function of depth and time with a constant thermal diffusivity of 0.00212 cm^2/sec, a constant half amplitude of 2.655°C and a constant phase lag of 70.67 days.

Chapter 7

THERMAL CONDUCTIVITY OF SEDIMENTS UNDER A HAWAIIAN ALPINE LAKE

A two-meter core sample from the sediment layer between 3 and 5 meters below Lake Waiau's surface was obtained at the temperature-probe measurement site by A. H. Woodcock on 5 May 1967. A more specific location of the selection site is shown in Figure 6-1. Two specimens were sliced from the ends of this core, one from the 3-meter and the other from the 5-meter level. These samples were both placed inside a cast acrylic annulus, shown in the photographs of Figure 7-1. A slight remolding of the specimen's original shapes was necessary for the fit into the annuluses. The annuluses are needed to support the 15.2 kg weight as the samples are being measured with the apparatus and method outlined in Chapter 3.

The annuluses have an inside diameter of 4.420 cm and an outside diameter of 5.080 cm. The manufacturer's specifications show the thermal conductivity of cast acrylic to be 0.00045 cal/sec cm °C. If we assume that the upper and lower copper discs maintain constant temperatures of 75°C and 35°C, respectively, over a time interval of 3.5 hours and the thermal conductivity of the sediment sample is 0.0025 cal/sec cm °C with a thickness of 1.6 cm, then the heat loss to the annulus is estimated to be 5.4% of the heat flow between the copper discs. With the estimated heat loss for the apparatus as calculated in Chapter 3, the total heat loss in the measurement of the sediments is approximately 8.5%. The heat-flux values computed for the thermal-conductivity measurements have been adjusted to compensate for this loss.

The results, corrected for heat loss, of the thermal-conductivity

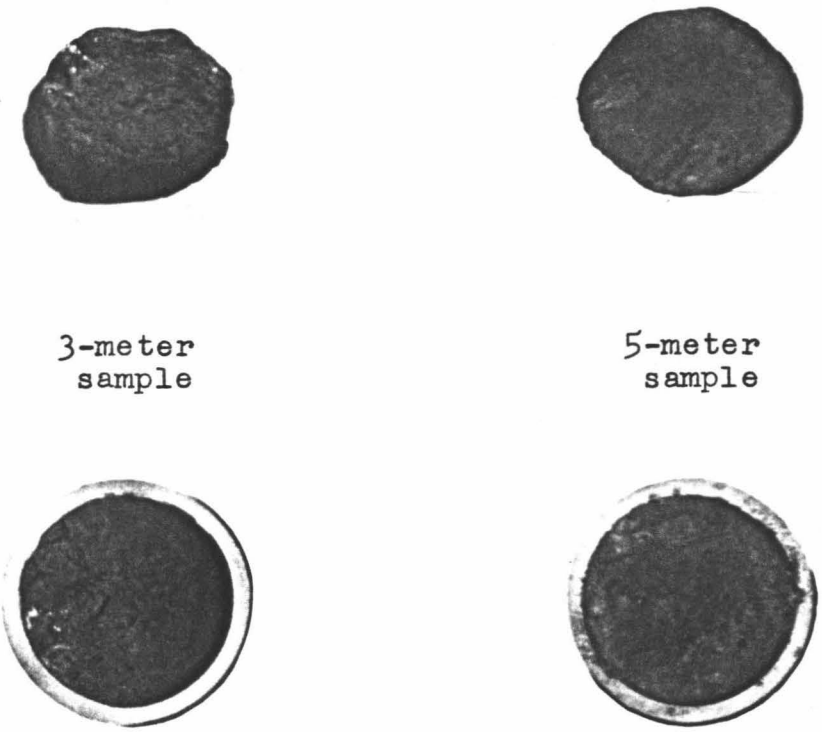

Figure 7-1. Specimens sliced from a two-meter core sample of Lake Waiau's sediment. The upper pictures are the specimens as received from A. H. Woodcock and the lower pictures are the same specimens remolded into plexiglass annuluses.

measurements using the steady-state apparatus are listed in Table 7-1 and Table 7-2. Regression equations from these computations are plotted on Figure 7-2. The notable feature of this plot is the large difference in the temperature dependence between the two samples. It is negligible in the 3-meter sample, but it is very pronounced in the 5-meter sample. An explanation of this observation follows.

The samples were inspected between individual measurements as part of the procedure. As the measurements progressed, the sediment sample was observed to shrink slightly within the annulus, indicating desiccation. Desiccation is quite possible since the temperature of the upper surface of the soil disc is maintained around 70°C and the apparatus encasement is not air-tight. The 5-meter sample was measured before any shrinkage was observed. It was also thicker, which indicates that more axial shrinkage should occur. The axial shrinkage would increase the contact resistance with the upper copper-disc since the annulus restrains the copper discs to a constant separation. A discussion of the contact-resistance problem in Chapter 3 illustrates the effect it has on the temperature at the contact surfaces. In this apparatus it causes the measurement of the temperature gradient to be too large, thus decreasing the computed thermal-conductivity value. The trend should be for the later measurements to have lower values, which is shown to be true in Table 7-2. Thus, the measurements of the 5-meter sample are considered unreliable for the later times. The mean of the first four measurements is 0.0029 cal/sec cm °C and is now considered the thermal-conductivity measurement of the 5-meter sample.

The 3-meter sample was purposely made thinner and the sediment

Table 7-1. Thermal-conductivity measurements of a sediment sample from 3-meters below the surface of Lake Waiau.

Date	Time of Day	Ambient Air Temperature (°C)	Sample Mean Temperature (°C)	Thermal Conductivity (cal/sec cm °C)
4Apr75	2045	25.2	50.32	0.0025
5Apr75	0845	22.8	50.95	0.0023
5Apr75	1300	25.0	52.96	0.0023
5Apr75	1705	25.9	52.94	0.0022
5Apr75	2115	24.8	49.78	0.0026
6Apr75	0640	23.0	33.47	0.0023
6Apr75	0950	23.4	34.14	0.0025
6Apr75	1300	25.1	32.90	0.0023
6Apr75	1600	25.8	32.69	0.0025
6Apr75	1915	26.0	31.70	0.0024

Regression equation: $k = 2.5 - 0.001\ T$ mcal/sec cm °C

Standard error of estimate = 0.12 mcal/sec cm °C

Mean reproducibility error = 3.6%

Sample disc thickness = 1.240 cm

Sample surface area = 15.459 cm^2

Table 7-2. Thermal-conductivity measurements of a sediment sample from 5-meters below the surface of Lake Waiau.

Date	Time of Day	Ambient Air Temperature (°C)	Sample Mean Temperature (°C)	Thermal Conductivity (cal/sec cm °C)
28Mar75	1620	23.5	58.29	0.0031
29Mar75	1025	23.0	57.85	0.0028
29Mar75	1550	25.1	53.66	0.0029
29Mar75	2130	24.6	54.65	0.0029
30Mar75	0715	23.4	43.42	0.0021
30Mar75	1030	24.9	42.12	0.0020
30Mar75	1305	26.8	40.80	0.0020
30Mar75	1625	27.7	42.70	0.0020
30Mar75	2120	27.3	50.82	0.0024
30Mar75	2330	25.5	40.93	0.0022

Regression equation: $k = - 0.33 + 0.06\ T$ mcal/sec cm °C

Standard error of estimate = 0.12 mcal/sec cm °C

Mean reproducibility error = 3.9%

Sample disc thickness = 1.648 cm

Sample surface area = 15.459 cm^2

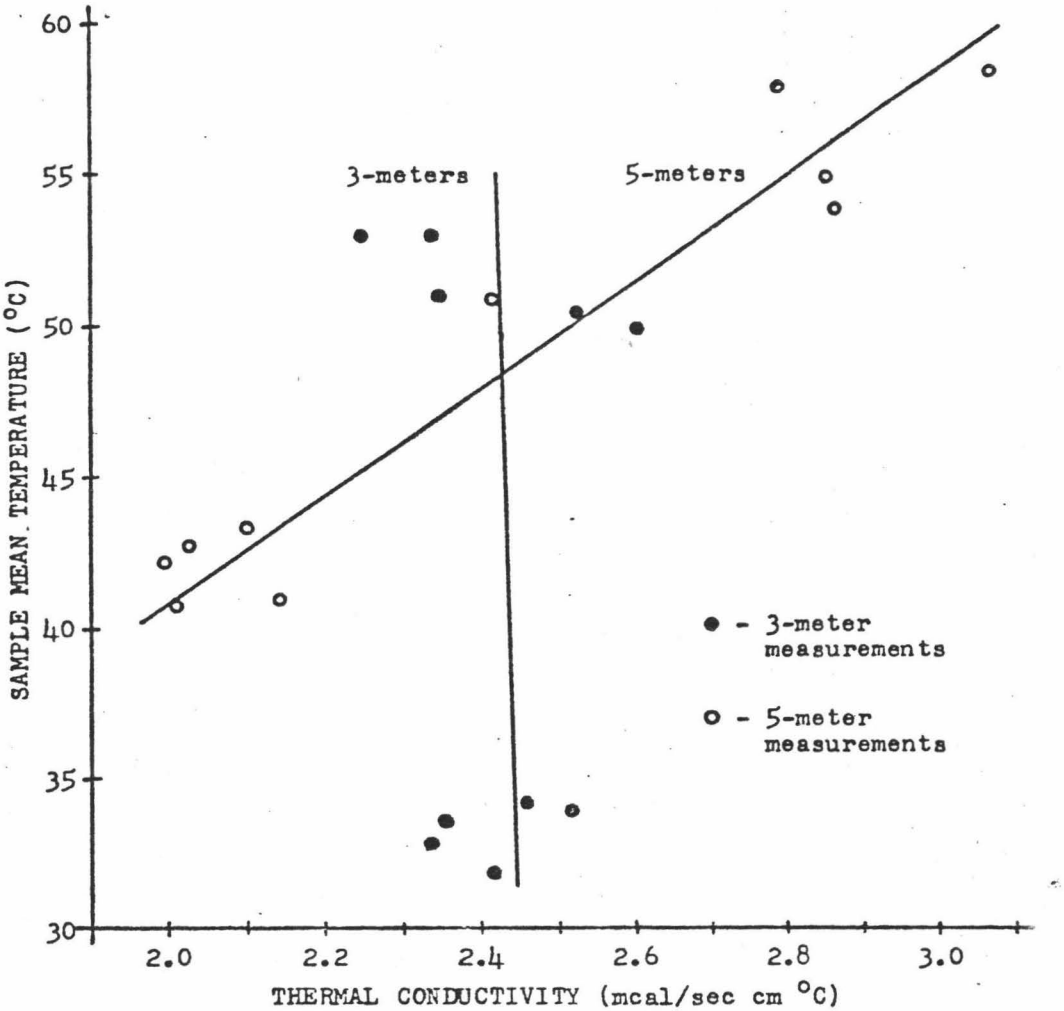

Figure 7-2. Graph of regression lines for the sample mean temperatures fitted to the thermal conductivity measurements of samples obtained from Lake Waiau sediment.

molded into the annulus was increased slightly to account for the shrinkage effect. The mean value of the thermal-conductivity measurements for the 3-meter sample is 0.0024 cal/sec cm °C. The difference between the steady-state measurements of the 3-meter and the 5-meter levels is 20%.

Upon completion of the thermal-conductivity measurements by the steady-state apparatus, the samples were weighed several times in the series of steps outlined by Lambe (1951) to determine the particle density and the moisture content of the samples. The mean particle density was found to be 2.40 gm/cm^3 and the moisture content of the sample from the 3-meter sample was 76.7%. The bulk density for the 3-meter sample is computed to be 1.36 gm/cm^3. The core sample was not stored in a sealed container over the past eight years, therefore, the moisture-content value cannot be representative of the 'in situ' situation.

Woodcock and Groves (1969) report values of moisture content at the 4-meter and the 6-meter levels to be 74% and 48%, respectively. This indicates that the moisture content decreases with increasing depth. The varying amounts of water with respect to the sediment particles will cause the bulk density and the specific heat of the sediment to also vary with depth. These parameters are involved in the conversion of thermal diffusivity to thermal conductivity through the relation

$$k = D\rho c \qquad (5.1)$$

mentioned in Chapter 5.

If we take the thermal diffusivity to be 0.00212 cm^2/sec, as measured, the particle density as 2.40 gm/cm^3, as measured, and assume the specific heat of the soil particles to be 0.22 cal/gm °C, then the cor-

Table 7-3. For fixed thermal diffusivity and constant particle density, variation of thermal conductivity versus moisture content.

Moisture Content (%)	Bulk Density (gm/cm^3)	Specific Heat (cal/gm °C)	Thermal Conductivity (cal/sec cm °C)
74*	1.81	0.522	0.00212
61	1.87	0.516	0.00205
48*	1.95	0.473	0.00196

* Moisture-content values reported by Woodcock and Groves (1969).

responding values of bulk density, specific heat and thermal conductivity are given in Table 7-3 for three values of moisture content (weight percentage). This table shows that for decreasing moisture content, the bulk density increases, and the specific heat and thermal conductivity both decrease. However, within the moisture content limits of 48-74%, the thermal conductivity varies about the value 0.00205 cal/sec cm °C differing by no more than 4.3%.

The measurements made by the steady-state apparatus differ from the above estimate by 18% and 41%. This difference can be accounted for, in part, by the remolding that was necessary to fit the sample into the annuluses. Also, small slices from within the core sample are probably not representative of the entire sediment layer. The insulating effect of the ash layers is not included in the laboratory measurements. The most representative value for the 'in situ' thermal conductivity of the sediments of Lake Waiau found in this study is 0.00205 cal/sec cm °C.

The negative thermal gradient determined by Woodcock and Groves (1969) is 0.052 °C/m. If we combine this value with the thermal-conductivity estimate above, we obtain a heat flux of 0.0107 cal/sec m^2 downward through the sediments at the area of the lake from which the measurements were taken, shown in Figure 6-1.

Chapter 8

DISCUSSION OF RESULTS, CONCLUSIONS AND SPECULATIONS

The finding of a significant transverse anisotropy in basalt contradicts a report by Horai and Baldridge (1972). They state that the pulverization of specimens, from macroscopically isotropic and homogeneous igneous rock, has negligible effects on the thermal-conductivity properties of the rock. The specimen obtained from the Sugarloaf lava flow (Figures 4-3 to 4-5) is macroscopically isotropic and homogeneous, consequently it would qualify as a candidate for pulverization according to the above criteria. If this specimen were pulverized into a powder before the thermal conductivity was measured, the results would differ from those obtained by the steady-state apparatus in this study. The loss of the 29% difference in the thermal conductivity at two orientations within this specimen would not be trivial.

The importance of transverse anisotropy of thermal conductivity in rocks has been indicated by Heiland (1963, p. 852), who has analyzed the effect transverse anisotropy has on the geothermal gradient in dipping layers of rock. He cites two areas where this effect is significant; Salt Creek dome, Wyoming and the geologic section between Oklahoma City and Sapulpa. The geothermal step (reciprocal of the geothermal gradient) was found to increase 10 feet per °C for a change in dip from 0° to 30° in slate with a factor of transverse anisotropy of 1.765.

There are a number of ways the work accomplished in this study could be improved upon. The specimen of glass was measured as a test case with results very near the precise measurements made on fused quartz by Sugawara (1968). A better means of calibrating this and other

similar apparatus would be to obtain a standard specimen with a known thermal conductivity. Ratcliffe (1959) mentions two commercial firms where standard specimens can be obtained: Quartz Crystal Company, New Malden, England and Thermal Syndicate Limited, Wallsend, England.

The accuracy of the thermal-conductivity measurements could be improved by using finite-element analysis to define the heat losses in the apparatus. The heat loss has been estimated to be 3.15% for the glass measurement using steady-state analysis. The finite-element method would be more appropriate since the problem could be modeled in the transient state. The contact resistance could also be incorporated into the model and a more precise value for the heat flow through the sample could be obtained.

The problem of contact resistance was encountered in the Sugarloaf lava measurements due to the glycerin being absorbed by the rock samples. A suggested method to overcome this problem when measuring porous specimens would be to use gold foil, instead of glycerin, at the contact interfaces. Sugawara (1968) used gold foil as a contact medium, although he does not mention how it would be beneficial for porous specimens. Gold is very malleable and under pressure it would tend to shape itself to the asperities of the contact interface, thus, reducing the contact resistance without being lost to the pores of the sample.

The estimate of the thermal diffusivity of the Lake Waiau sediments could be improved upon by incorporating another parameter into the new method. The annual temperature wave was assumed to be a sine wave with a period of 365 days, which is not the case in reality. A more realistic driving function could be modeled into the method from the continu-

ous temperature data that is monitored at the Mauna Kea weather station.

Conclusions.

From the results of the steady-state thermal-conductivity measurements on a sample from the Sugarloaf lava flow in the first part of this study, it was concluded that a transverse anisotropy of 0.78 exists in this sample. The cause of the anisotropy is apparently due to compositional variations of the minerals rather than any structural alignment of crystals within the rock mass. Subsequent studies should include measurements on samples taken from selected locations across the whole layer to examine the possible existence of transverse anisotropy throughout the entire lava flow.

The objective of the second part of this study, as stated in Chapter 5, was to obtain a value for the thermal conductivity of the sediments under Lake Waiau. This was accomplished by estimating the thermal diffusivity to be 0.00212 cm^2/sec using an improved method applied to temperature data collected by A. H. Woodcock. The thermal conductivity of these sediments is derived from this estimate to be 0.00205 cal/sec cm °C. This result combined with the results of Woodcock and Groves (1969) indicates a heat flux of 1.07 μcal/sec cm^2, downward, flows through the 4-meter layer of sediments in the center of the lake.

Speculations.

It is also worth while to note that anisotropy of thermal conductivity is not considered in most heat-flux measurements. For instance, the heat flow over the oceans is often determined from thermal-conduc-

tivity measurements with a needle-probe apparatus of core samples from the ocean sediments. The needle-probe is inserted into the core normal to the cylindrical axis. The measurement then represents an average of two thermal-conductivity values; one parallel and the other normal to the cylindrical axis of the core. Consequently, if transverse anisotropy exists in the core samples, as we would expect in laminated sediments, it will not be measured with a needle-probe apparatus alone. A suggested method of discerning the significance of transverse anisotropy in core samples from sediments with minimal sample fabrication follows.

If the needle-probe were inserted into the core sample parallel to the cylindrical axis, it would then measure the average thermal conductivity normal to the axis. For most core samples, those with the cores taken normal to the sediment bedding planes, this measurement would represent the thermal-conductivity value parallel to the layering. From a selected slice of the core, the thermal conductivity parallel to the core axis (normal to the layering) could be measured with a steady-state apparatus similar to the one used in this study. Then the difference between these two measurements would determine the significance of the transverse anisotropy in the sediments.

Another practical use for the apparatus used in this study is in the geothermal exploration for exploitable geothermal resources. The cost of a geothermal-gradient survey across a promising geothermal area is estimated by Kappelmeyer and Haenel (1974, p. 137) to be $1,300,000 U.S. currency. The cost of the apparatus built for this study could be under $1000. A millivoltmeter could be used equally well in place of the strip-chart recorder and a single power-supply unit instead of the

dual model is adequate. For less than 0.1% of the total cost of a geothermal-gradient survey, a laboratory capability for obtaining thermal-conductivity values is then possible. Incorporating the thermal-conductivity capability into the geothermal-gradient survey could convert the work into a heat-flux survey: the heat-flux values have been shown in Chapter 1 to be more reliable indicators of economically exploitable geothermal reservoirs than geothermal-gradient values alone.

Appendix A

Serial equipment used with the steady-state apparatus:

1. Hewlett Packard dual D. C. power supply, model 6227B, serial number: 1146A-01634.

2. Hewlett Packard strip-chart recorder, model 7100BM-19-23, serial number: 1148A06006.

3. Hewlett Packard input modules, model 17505A, serial numbers: 1210A00348 and 1210A00349.

Appendix B

Computer program used in the improved estimate of thermal diffusivity:

MAIN.

```
      DIMENSION T(147),T1(147),Y(147)
      N=147
      DO 5 I=1,N
      READ(5,10) TI(I),Y(I),T(I)
5     Y(I)=Y(I)-3.0
      TR=1.5
      DO 25 L=1,8
      PHI=45.0
      TR=TR + 0.2
      WRITE(6,45) TR
      DO 25 J=1,10
      WRITE (6,35)
      PHI=PHI + 2.0
      A=0.009
      DO 25 K=1,20
      A=A + 0.001
15    SS=0.0
21    DO I=1,N
      S=(T(I)-TEMP(Y(I),TI(I),A,PHI,TR))
      S=S*S
20    SS=SS + S
      WRITE(6,30) SS,A,PHI
25    CONTINUE
10    FORMAT (3F10.3)
30    FORMAT (' ','SS = ',1PE13.6,5X,'A =',1PE13.6,5X,'PHI =',
     .        1PE13.6)
35    FORMAT (1X,/)
45    FORMAT (1H1,'TR = ',1PE13.6,//)
40    STOP
      END
```

TEMP.

```
      FUNCTION TEMP(Y,TI,A,PHI,TR)
      PI=3.1415928
      P=365.0
      TM=6.3
      E=2.71828
      FAC1=-SQRT(PI/(A*P))
      FAC2=2*PI/P
      TEMP=E**(FAC1*Y)
      TEMP=TR*TEMP
      TEMP=TEMP*SIN(FAC2*(TI + PHI) + FAC1*Y) + TM
      RETURN
      END
```

REFERENCES CITED

Abeles, B., G. D. Cody, and D. S. Beers. "Apparatus for the Measurement of Thermal Diffusivity of Solids at High Temperatures". Journal of Applied Physics. vol. 31, no. 9, pp. 1585-1592, 1960.

Adams, William Mansfield. "The Prospect of Finding Exploitable Geothermal Reservoirs". Unpublished paper. University of Hawaii, 1975.

Birch, Francis and Harry Clark. "The Thermal Conductivity of Rocks and its Dependence upon Temperature and Composition". American Journal of Science. vol. 238, pp. 529-558 and pp. 613-635, 1940.

Carslaw, H. S. and J. C. Jaeger. Conduction of Heat in Solids. Second edition. Published by Oxford at the Claredon Press, 1959.

Cowan, Edward. "Geothermal Power Hunted in Montana". New York Times. page 55, June 9, 1974.

Fried, E. "Thermal Conductivity Contribution to Heat Transfer at Contacts". Thermal Conductivity. vol. 2, pp. 253-274. Edited by R. P. Tye, Academic Press, 1969.

Hammond, Allen L., William D. Metz and Thomas H. Maugh II. "Energy and the Future". American Association for the Advancement of Science, 1973.

Heiland, C. A. Geophysical Prospecting. Hafner Publishing Company, 1963.

Horai, Ki-iti and Seiya Uyeda. "Studies of the Thermal State of the Earth. The Fifth Paper: Relation between Thermal Conductivity of Sedimentary Rocks and Water Content". Bulletin of the Earthquake Research Institute. vol. 38, pp. 199-206, 1960.

Horai, Ki-iti. "Thermal Conductivity of Rock-Forming Minerals". Journal of Geophysical Research. vol. 76, no. 5, pp. 1278-1308, 1971.

Horai, Ki-iti and Scott Baldridge. "Thermal Conductivity of Nineteen Igneous Rocks, II Estimation of the Thermal Conductivity from Mineral and Chemical Compositions". Physics of Earth Planet Interiors. vol. 5, pp. 157-166, 1972.

Lambe, William T. Soil Testing for Engineers. John Wiley and Sons, Incorporated, 1951.

Lovering, T. S. and H. D. Goode. "Measuring Geothermal Gradients in Drill Holes Less than 60 Feet Deep, East Tintic District, Utah". U. S. Geological Survey Bulletin No. 1172, 1963.

Kappelmeyer, O. and R. Haenel. "Geothermics with Special Reference to Application". Geoexploration Monographs Series 1 - No. 4. Gebrüder Borntraeger, 1974.

Kirkham, Don and W. L. Powers. Advanced Soil Physics. Wiley-Interscience, 1972.

Misener, A. D. and A. E. Beck. "The Measurement of Heat Flow over Land". Methods and Techiques in Geophysics. Edited by S. K. Runcorn, 1960.

McNitt, James R. "Review of Geothermal Resources". Chapter 9, AGU 1288, Terrestrial Heat Flow. Edited by W. H. K. Lee, 1965.

Ratcliffe, E. H. "Thermal Conductivities of Fused and Crystalline Quartz". British Journal of Applied Physics. vol. 10, pp. 22-25, 1959.

Reiter, Marshall and Harold Hartman. "A New Steady-State Method for Determining Thermal Conductivity". Journal of Geophysical Research. vol. 76, no. 29, pp. 7047, 1971.

Robertson, Eugene C. and Dallas L. Peck. "Thermal Conductivity of Vesicular Basalt from Hawaii". Journal of Geophysical Research. vol. 79, no. 32, pp. 4875-4888, 1974.

Stearns, H. T. "Geologic Map and Guide of the Island of Oahu, Hawaii". Hawaii Division of Hydrology Bulletin 2. pp. 75, 1939.

Sugawara, Akira. "The Precise Determination of Thermal Conductivity of Pure Fused Quartz". Journal of Applied Physics. vol. 39, no. 13, pp. 5994, 1968.

Tomovic, Rajko. Sensitivity Analysis of Dynamic Systems. McGraw-Hill, 1963.

Touloukian, Y. S., R. W. Powell, C. Y. Ho and P. G. Klemens. "Thermal Conductivity - Nonmetallic Solids". Thermophysical Properties of Matter. vol. 2, 1970.

Von Herzen, R. and A. E. Maxwell. "The Measurement of Thermal Conductivity of Deep-Sea Sediments by a Needle-Probe Method". Journal of Geophysical Research. vol. 64, no. 10, pp. 1557-1563, 1959.

Winchell, Horace. "Honolulu Series, Oahu, Hawaii". Bulletin of the Geological Society of America. vol. 58, pp. 1-78, 1947.

Woodcock, Alfred H., Meyer Rubin and R. A. Duce. "Deep Layer of Sediments in an Alpine Lake in the Tropical Mid-Pacific". Science. vol. 154, no. 3749, pp. 647-648, 1966.

Woodcock, A. H., and Gordon W. Groves. "Negative Thermal Gradient under an Alpine Lake in Hawaii". Deep-Sea Research. Supplement to vol. 16, pp. 393-405, 1969.